ON THE IMPACT OF SPACE-BASED OBSERVING SYSTEMS IN
THE JMA GLOBAL FORECAST/ANALYSIS SYSTEM

K.Kashiwagi
Japan Meteorological Agency
Tokyo, Japan

1.   OUTLINE OF THE DATA ASSIMILATION SYSTEM

The twelve-hour intermittent global data assimilation system was put into

operation on 1 March 1984. In the following, we briefly describe the major

functional components of the system.

1.1   Pre-analysis

Observational data received from the GTS are decoded according to their code

forms. Data to be used in the analysis are SYNOP, SHIP, TEMP, PILOT, AIREP,

SATEM, SATOB, DRIBU, COLBA, Australian PAOB and GMS digital cloud data. These

data are sorted into 2.5 degree latitude-longitude boxes.

A check of climatological reasonability is performed for all types of data.

Vertical consistency checks (for example - check of temperature lapse rate,

check of hydrostatic relationship, check of consistency between the data at

mandatory levels and the data at significant levels) are performed for TEMP

and PILOT data using Parts A,B,C and D, and SYNOP data. Furthermore, solar

radiation corrections are made for TEMP data above the 150 mb level. A lapse

rate check for SATEMs is also performed using the mean virtual temperature

calculated from the thickness.

1.2   Analysis

After horizontal consistency checks have been performed, the analysis is
carried out on the 2.5 degree latitude-longitude grid system at 15 levels.
The analysed variables are geopotential height, wind components, temperature
and dewpoint depression (below 400 mb). Details of the analysis system are
given in Sects. 3 and 4.

1.3   Post-analysis

The different vertical coordinate systems used in the analysis and prediction
model necessitates a pressure to sigma coordinate conversion. A cubic spline
is used for the vertical interpolation of winds and heights, and temperatures
at the sigma levels are obtained from the vertical derivatives of the fitted
heights. Simple linear interpolation is used for dew point depressions.

The transformation from analysis grid to spectral components is carried out
using a Fast Fourier Transform.

1.4   Prediction

Preceding the twelve-hour forecast, a nonlinear normal mode initialization
procedure is applied to suppress the gravity wave noise. A 12-level global
spectral model is used to create the first guess for the tropospheric
analysis. The model has a horizontal resolution of triangular 42 truncation
and incorporates full physical processes, including the diurnal variation of
shortwave radiation and cloud effects. The predicted fields are converted to
the guess fields through the inverse process of post-analysis. Further
details of the forecast model can be found in Kanamitsu et al. (1983).

2. TREATMENT OF DATA

The cut-off time is 6 hours after the analysis time and all the data within ±6 hours of analysis time are used. Off-time data are used without any locational correction, but the observation errors are changed according to the time difference from the analysis time.

Data at only the mandatory pressure levels are used for TEMPs and PILOTs, and AIREPs and COLBAs are assigned to the nearest analysis level. SATOBs at low levels (900 mb $\geqslant$ P_t (reported pressure level in SATOB) $\geqslant$ 650 mb) are assigned to the 850 mb level whilst SATOBs at high levels (350 mb $\geqslant$ P_t $\geqslant$ 70 mb) are used in the analysis at 300, 250, 200 and 150 mb. Because of their large negative bias near the jet stream, SATOBs at high levels poleward of 30 degrees are not used in the analysis.

The SATEM thicknesses are converted into temperatures at the analysis levels using a cubic spline; they are also converted into geopotential heights. The following procedure is used to reduce the biases caused by the rather strong vertical correlation of their observational errors. First, we calculate the thickness between two analysis levels from the SATEM data. Next, we add this thickness to the value of the analysed height from the level below to give the height at the next level.

Total cloud amount, mean cloud top temperature and its standard deviation over a one degree latitude-longitude box are obtained from GMS observations. Vertical profiles of dew point depression are estimated using the statistics pre-determined by comparing these parameters with collocated sonde observations.

If more than two observations of the same type are located within a specified distance, only one observation is selected according to the observation time and the specified relative confidence; this is done in order to avoid a strongly localized analysis. The specified distance is 50 km for the surface data (SYNOP, SHIP, DRIBU), AIREPs and SATOBs. The nominal horizontal resolution of SATEMs is about 200 km and their observation errors are much larger than those for the sondes. Therefore, the specified distance for SATEMs is 200 km, and so SATEMs within 200 km of TEMPs are not used. This large distance for SATEMs is necessary to avoid computational instability caused by the horizontal correlation of observation error when solving the normal equations.

3.   ANALYSIS OF TROPOSPHERE (BELOW 100 MB)

3.1   Formulation of analysis model

Our tropospheric analysis scheme is based on the optimum interpolation method. The interpolated value at a grid point is estimated by

$$F^I_g = F^p_g + \sum_{i=1}^{n} w_i \ (F^o_i - F^p_i)\sigma^p_g/\sigma^p_i \qquad (1)$$

where F denotes any meteorological variable, n the number of variables used in the analysis, w the weights to be determined and σ^p the prediction error standard deviation. Superscripts o, p and I indicate observed, predicted and interpolated values, respectively, subscript g the grid point and the variable to be analysed, and subscript i the observation point and the variable used in the analysis.

In general, F^I_g in Eq.(1) will not give the true value at the grid point, but will differ by an amount called the analysis error. The weights are determined from the condition that the mean square analysis error $(E^I_g)^2$ over a large number of analysis situations be a minimum. Because observations are usually made with no knowledge of the predicted values, the prediction errors and observation errors are assumed to be uncorrelated. Then the requirement $\partial(E^I_g)^2/\partial w_i = 0$ produces a set of equations (normal equations), i.e.,

$$\sum_{j=1}^{n} (\mu^p_{ij} + \mu^o_{ij} \lambda_i \lambda_j) \ w_j = \mu^p_{ig} \qquad (i=1,2,...n) \qquad (2)$$

$$\lambda_i = \sigma^o_i/\sigma^p_i$$

where μ^p and μ^o denote prediction and observation error correlation coefficient respectively, and σ^o is the observation error standard deviation.

In principle, F_i in Eq.(1) can be different from F_g with regard to the type of variable, vertical level and time. A two-dimensional form is used in our system because of operational time limits.

The form of the analysis method depends upon the latitude (ϕ). Over the extratropical region ($|\phi| \geqslant 15°$), a multivariate method is used for the analysis of height and wind at upper levels. However, over the subtropical region ($15° \leqslant |\phi| \leqslant 25°$), the wind-height correlations are multiplied by an empirical coefficient which depends on latitude in order to gradually decouple the wind and height analysis. Over the tropics ($|\phi| < 15°$), where the geostrophic relation is inappropriate, winds are analysed using a bivariate method, and the geopotential heights are analysed by a univariate method at the upper levels.

In the northern hemisphere, sea level pressure and wind are analysed by the univariate method. However, over the extratropical region of the southern hemisphere, which is mostly covered by the ocean, they are analysed by a multivariate method because the main data sources are the sea level pressure from PAOBs or DRIBUs.

Temperature and dew point depression are analysed by a univariate method everywhere.

3.2   Determination of statistical parameters

Under the assumption of homogeneity and isotropy, the prediction error auto-correlation for height, temperature and dew point depression are modelled by the formula

$$\mu_{ij}^{p} = \exp\left(-br_{ij}^{2}\right) \tag{3}$$

where b is a constant which depends on variable, level and latitude, and r_{ij} the distance between points i and j. First, we calculate the apparent

prediction error correlations (correlations of the difference between prediction and observation) for many pairs of observation points over East Asia, United States of America, Europe and Russia. Then, using these correlations, the values of b are calculated by the same procedure as used by Alaka and Elvander (1972) except for the functional form of the correlation function. After some trial analysis experiments, the values of b shown in Fig. 1 were determined.

The wind-wind and wind-height prediction error correlations over the extratropical region are derived from the height-height correlation using the geostrophic relation. Using Eq.(3) for the height-height correlation, the following relations are obtained.

$$\mu^P(z_i u_j) = - \sqrt{2b} \ (y_i - y_j) \ \mu^P(z_i z_j)$$

$$\mu^P(z_i v_j) = - \sqrt{2b} \ (x_i - x_j) \ \mu^P(z_i z_j)$$

$$\mu^P(u_i u_j) = \left\{ 1 - 2b \ (y_i - y_j)^2 \right\} \mu^P(z_i z_j) \tag{4}$$

$$\mu^P(v_i v_j) = \left\{ 1 - 2b \ (x_i - x_j)^2 \right\} \mu^P(z_i z_j)$$

$$\mu^P(u_i v_j) = \ 2b \ (x_i - x_j)(y_i - y_j) \mu^P(z_i z_j)$$

where $\mu^P(F_i G_j)$ denotes the prediction error correlation between variable F at point i and variable G at point j.

In the tropics, the wind-wind correlations are derived from the stream function correlation under the assumption of nondivergent flow. These correlation coefficients have the same form as in Eq.(4) except that $\mu^P(z_i z_j)$ is replaced by $\mu^P(\psi_i \psi_j)$ where ψ is the streamfunction. We assumed that the values of b for $\mu^P(\psi_i \psi_j)$ are the same as for $\mu^P(z_i z_j)$.

The observation error correlation of SATEMs is also modelled by Eq.(3), but

b=11.3 x 10^{-6} km^{-2} is used (Bergman, 1979). No observation error correlations

are assumed for the other types of data.

The observation error standard deviation for sonde data was modelled by

referring to papers on this subject (Kurihara (1961), Lenhard (1970)) and by

considering the following statistics.

(1)   RMS differences between observation and analysed value over the data

        rich regions.

(2)   RMS and correlation of the apparent prediction error.

The observation error standard deviation for other types of data and the

prediction error standard deviation are modelled using the RMS differences

betweeen other observations or predictions and the collocated sonde data.

Fig. 2 shows the values of these parameters used in the model.

3.3   Data selection procedure

The data selection procedure and the maximum number of data to be used at one

grid point were decided from some trial analyses using real data, and model

experiments using idealized observation networks. Boxes with sides of 5, 10,

15, 20, 25 and 30 degrees of latitude, centred on the grid point, are scanned

until the M closest variable are selected or the largest box is scanned. The

scanning for each grid point is started from the box size pre-determined by

the statistics of data distribution. M is set to 10 in the univariate case

and varies from 30 at lower levels to 45 at upper levels in the multivariate

case. All the variables at one observation point are simultaneously used in

the multivariate case. If there is only one or no observation point in the
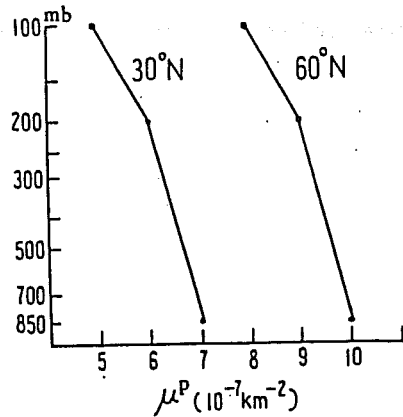
largest box, the guess value is used.

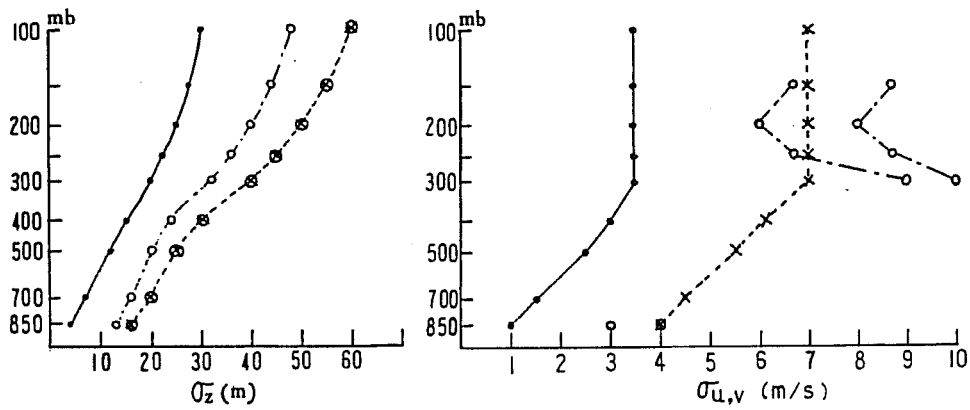Fig.1 The value of b in Eq.(3) for height-height prediction error correlation.

Fig.2 Observation and prediction error standard deviation for height (left) and wind (right).
●———● sonde observation, ✕----✕ prediction
○—·—○ satellite observation (min. and max.)

3.4   Quality control of data

A gross error check and horizontal consistency check are performed. The residual (D) from the guess value is calculated for every observation. If $D > C_1$ the data are rejected, but if $C_1 > D > C_2$, the data are checked against the residual interpolated from the neighbouring observations. The data which do not agree within a reasonable tolerance with the interpolated values are rejected.

4.   ANALYSIS OF THE STRATOSPHERE (FROM 70 MB TO 10 MB)

Because there are only two sigma levels above the 100 mb level in our

operational forecast model, we cannot expect that the forecasts in the

stratosphere are as reliable as those in the troposphere. Therefore, analysis

methods which require forecast values as guess fields are not suitable in the

stratosphere. It is possible to use climatological values as guess fields,

however we consider that these are not suitable because the inter-annual

variation of physical fields is large in winter. Some data processing centres

use previously analysed fields as guess fields. In our opinion, there are few

theoretical arguments which justify the use of persistence as a guess field.

Therefore we consider that analysis methods without guess fields are more

suitable for the stratosphere than methods with guess fields.

We use the two-dimensional least squares fitting method for levels between

70 mb and 10 mb. The base functions are the products of the trigonometric

functions and spherical B-spline functions over the global domain. The

longitude dependent trigonometric functions are truncated at wavenumbers 6 to

8 and the latitude dependent spherical B-spline functions are differentiable

to the second order at the north and south poles. The distance between the

knot points which define B-spline functions is 10 degrees.

Temperature and height fields are fitted to the base functions by the least

squares fit method. Wind data, except in the tropics, are used in the height

analysis by assuming the geostrophic relationship. The method does not

require any guess fields; however we use the previously analysed values over

data sparse areas as pseudo-observations in order to avoid computational

instability.

Wind fields in the regions 90°N-30°N and 30°S-90°S are calculated from height fields using the geostrophic relation. Stream function fields in the tropics (30°N-30°S) are also fitted using wind data and pseudo-observations of stream function. The first pseudo-observations of stream function are calculated from height fields using the linear balance equation, where the non-zonal components of wind fields at the equator are forced to zero. Thereafter we use the previously analysed values as pseudo-observations. At the northern and southern boundaries, the analysed stream function fields are smoothly connected to the boundary values calculated from height fields by using the geostrophic relationship.

5. <u>DESIGN OF THE OBSERVING SYSTEM EXPERIMENTS</u>

We performed the observing system experiments (OSE) using our operational data assimilation system without any manual intervention. In the experiments we changed the assimilation cycle interval to 6 hours without any modification to the statistical parameters. Moreover, the solar radiation correction to sonde data was not performed because of the lack of statistics.

Our OSE, together with those performed at ECMWF and UKMO, comprise a triple OSE using an identical data set but different assimilation systems.

The data used in the experiments are decoded from the FGGE Main Level II-b data sets on magnetic tapes which were provided by ECMWF. The period for the OSE is from 27 February to 7 March 1979; this was chosen by ECMWF on the basis of the good data availability and interesting meteorological situation.

We started the OSE from the analysis at 00GMT 25 February in order to remove the strong influence of the first guess at the start. The 12-hour forecast fields from ECMWF Level III-b data at 12GMT on 24th was used as the guess fields for the first analysis.

Parellel sets of analyses were produced for the following three observing system configurations.

(1)   CONTL mode : All types of data are used.

(2)   NOSAT mode : Data derived from satellite observation are excluded.

(3)   SATEL mode : TEMP and PILOT data are excluded.

Furthermore, we carried out 10-day forecasts from OOGMT for every day of the period (9 cases). The CONTL analysis was extended to 17 March to verify the forecast. In this study we mainly compare the CONTL mode with the NOSAT mode; the SATEL mode was utilized to confirm the difference between the CONTL and NOSAT modes.

6.   STATISTICAL EVALUATION OF SATELLITE IMPACT ON THE ANALYSIS

Here we compare various statistics calculated from 18 analyses for 00GMT and 12GMT to investigate the overall characteristics of the impact of satellite data on the analysis.

6.1   Middle and high latitude over the northern hemisphere

Table 1 shows the average RMS differences between the analyses and sonde data. It indicates that the fit of the two analyses to sonde data are almost the same, not only over East Asia where satellite data are scarce at 00 and 12 GMT, but also over Europe where a large amount of satellite data are reported. The RMS difference between the CONTL and NOSAT analyses is shown in Fig. 3. Over the area where many sonde data are available the RMS values are at most 10 m and are smaller than the sonde observational error standard deviation. This is due to the following two facts; first we exclude SATEMs very close to sondes and secondly, the observation error assigned to SATEMs is 2-4 time larger than that assigned to sonde observations.

On the other hand, over oceanic areas the RMS differences between NOSAT and CONTL are very large. Fig. 4 shows the average difference between NOSAT and CONTL (i.e. bias of NOSAT mean height field from CONTL). It indicates that the negative bias in NOSAT causes the large RMS over the north Pacific. Although the biases exist through the whole layer, they are particularly large in the stratosphere. Fig. 5 shows the mean height field at 70 mb; note there is an erroneous low analysed in the stratosphere for the NOSAT case.

VARI-ABLE	AREA	MODE	LEVEL(mb) 850	700	500	300	200	100
Z(m)	E.ASIA	NOSAT	7.7	9.0	13.8	22.3	25.2	33.7
		CONTL	7.6	9.0	13.6	22.4	25.3	33.3
	EUROPE	NOSAT	7.8	10.0	16.2	26.5	33.0	42.5
		CONTL	7.8	9.9	16.4	26.3	33.0	42.1
U(m/s)	E.ASIA	NOSAT	2.4	2.5	3.2	4.5	4.5	3.4
		CONTL	2.4	2.5	3.2	4.5	4.2	3.4
	EUROPE	NOSAT	2.3	2.4	3.2	3.7	2.9	2.5
		CONTL	2.3	2.3	3.1	3.7	2.9	2.4
V(m/s)	E.ASIA	NOSAT	2.6	2.4	3.2	4.3	3.7	3.0
		CONTL	2.6	2.3	3.1	4.3	3.7	2.9
	EUROPE	NOSAT	2.4	2.5	3.4	4.1	3.3	2.6
		CONTL	2.3	2.5	3.4	4.1	3.3	2.5

Table 1   Average RMS of differences between analysis and sonde data.
Domains of abbreviated areas are as follows;
E.ASIA : 25N-50N, 105E-150E ; EUROPE : 45N-70N, 0E-60E
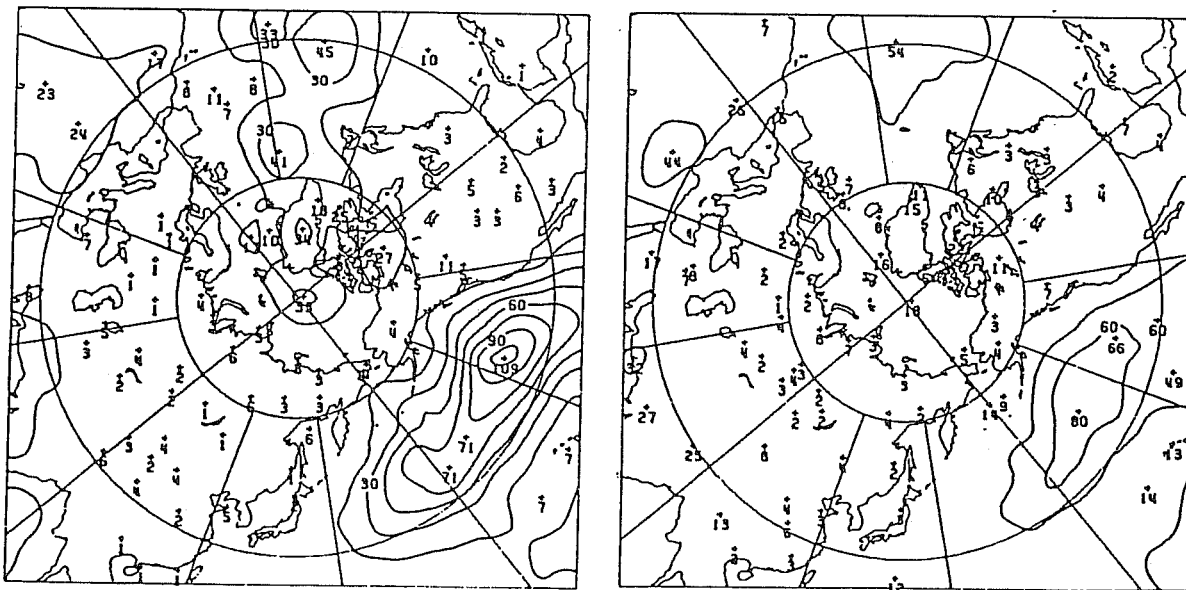
Fig.3   The RMS differences between CONTL and NOSAT height analysis
at 500mb (left) and 200mb (right).
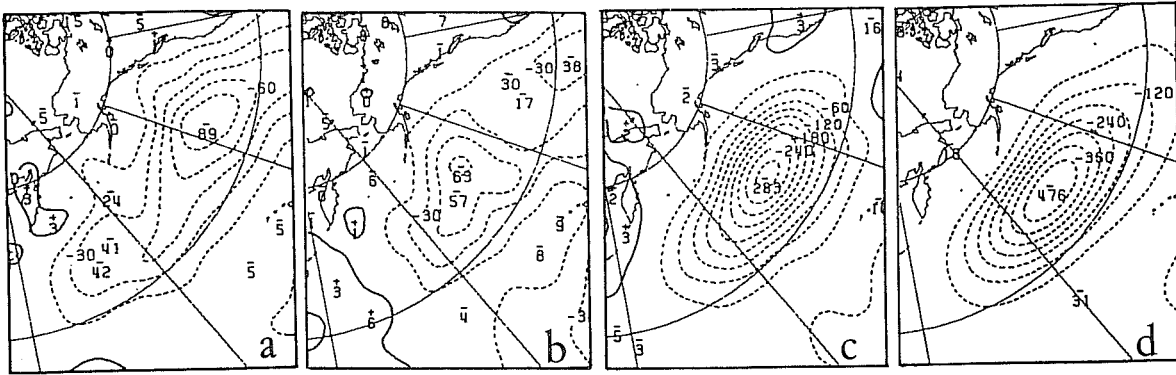
Fig.4 Differences (NOSAT minus CONTL) of mean analyzed height fields.
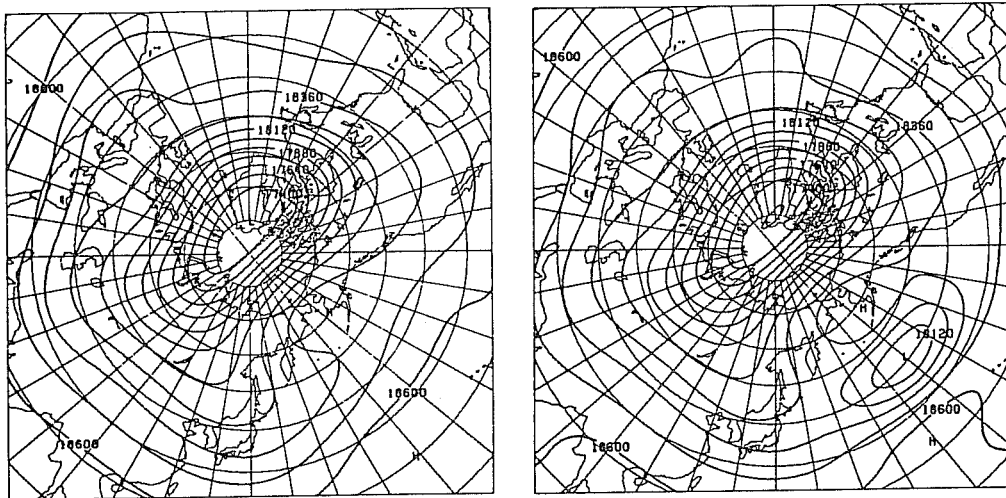(a) 500mb, (b) 200mb, (c) 100mb, (d) 70mb

Fig.5 Mean analyzed height fields at 70mb.
CONTL (left), NOSAT(right)

LEVEL (mb)	MODE	Z(m)				U(m/s)			
		E.ASIA	PACIFC	S.HEM	TROPIC	E.ASIA	PACIFC	S.HEM	TROPIC
850	NOSAT	6.2	24.9	50.1	9.6	1.4	5.2	6.5	3.9
	SATEL	22.9	13.7	19.7	9.9	4.6	3.6	4.1	3.5
	DIFF	-16.7	11.2	30.4	-0.3	-3.2	1.7	2.5	0.4
500	NOSAT	3.7	45.5	91.3	16.5	1.5	6.7	9.3	4.4
	SATEL	28.3	22.7	26.6	17.7	6.2	5.3	4.8	4.8
	DIFF	-24.7	22.8	64.7	-1.2	-4.8	1.4	4.6	-0.4
300	NOSAT	5.2	39.9	120.4	25.7	2.1	5.4	10.3	7.4
	SATEL	54.2	38.3	35.9	26.8	9.6	5.3	5.6	5.0
	DIFF	-49.0	1.6	84.5	-1.1	-7.5	0.1	4.7	2.5

Table 2 Area mean RMS of differences between individual
CONTL analysis and NOSAT and SATEL analyses
averaged over the 18 cases. See Table 4 for the
definition of areas.

We now trace the source of the negative biases in the stratosphere. The number of waves and the error assigned to the pseudo-observations in the analysis of the stratosphere are tuned by making an assumption about the availability of SATEMs over a wide area. When SATEMs are completely excluded for a long period, the analysis in the stratosphere is fitted locally to sonde data more and more, and may cause erroneous analysis over data void regions; for example, the maximum biase at 70 mb which is -130 m at 00GMT on the 25th repidly increases and becomes -415 m at 00GMT on the 27th.

The analysis in the stratosphere is independent of the forecast model because we do not use forecast results as guess fields there. However, the persistence of the negative biases in the stratosphere affects the analysis of the troposphere through the assimilation cycles. The biases in the stratosphere directly propagate to 100 and 150 mb through pressure to sigma and sigma to pressure interpolation procedures. The propagation to 200, 250 and 300 mb is rather slow and the magnitude of biases is considerably reduced, perhaps because there are many AIREPs at these levels. The reduction of biases at these levels weakens the propagation to the lower troposphere.

We performed another OSE using the analysis system in which the wave numbers of the stratospheric analysis are reduced. In this case, the negative biases in the stratosphere are greatly reduced; for example, the maximum mean biase at 70 mb becomes -124 m. Furthermore, the biases at all levels in the troposphere are also reduced over the area west of 210°E where the large biases in the stratosphere existed in the original NOSAT case. Almost all negative biases at levels from 100 mb to 250 mb are found to originate in the stratosphere.

On the other hand, the predominant biases at levels below 400 mb which exist over the area east of 210°E hardly change in this new OSE. The biases which result from the impact of satellite data are maintained and evolve through the assimilation system. The positions and magnitudes of the biases at these levels are not fixed in time. An example for the evolution of the biases in the troposphere is discussed in Sect. 8.

Table 2 displays the area mean RMS differences between CONTL and NOSAT analyses averaged over 18 cases. It is seen from Table 2 and Fig. 3 that the differences between NOSAT and CONTL around the 200-300 mb levels over the Pacific region are smaller than those above or below those levels over the north Pacific. Fig. 6 shows the RMS difference between the analysis and guess field. In SATEL, corrections to the guess values at 500 mb are smaller over the area where a small number of satellite data are available. On the other hand, the corrections at 200 mb are larger over this area because of the availability of AIREPs and/or SATOBs. The above results indicate that the wind and height fields are mutually influenced through the multi-variate analysis. Moreover the result suggests that the vertical structure of thickness temperature may be distorted above or below 200-300 mb when SATEM data are not used.

Fig. 7 shows the RMS difference between CONTL and SATEL for the 500 mb height analyses. It is found from Fig.6 that guess values in SATEL are corrected to the same extent as in CONTL over 0-90°E and 180-270°E where many SATEMs are available at 00GMT and 12GMT. Therefore, Fig.7 reveals that the difference between the CONTL and SATEL analyses over land in these areas are relatively small compared to those over other land areas. Over East Asia and the
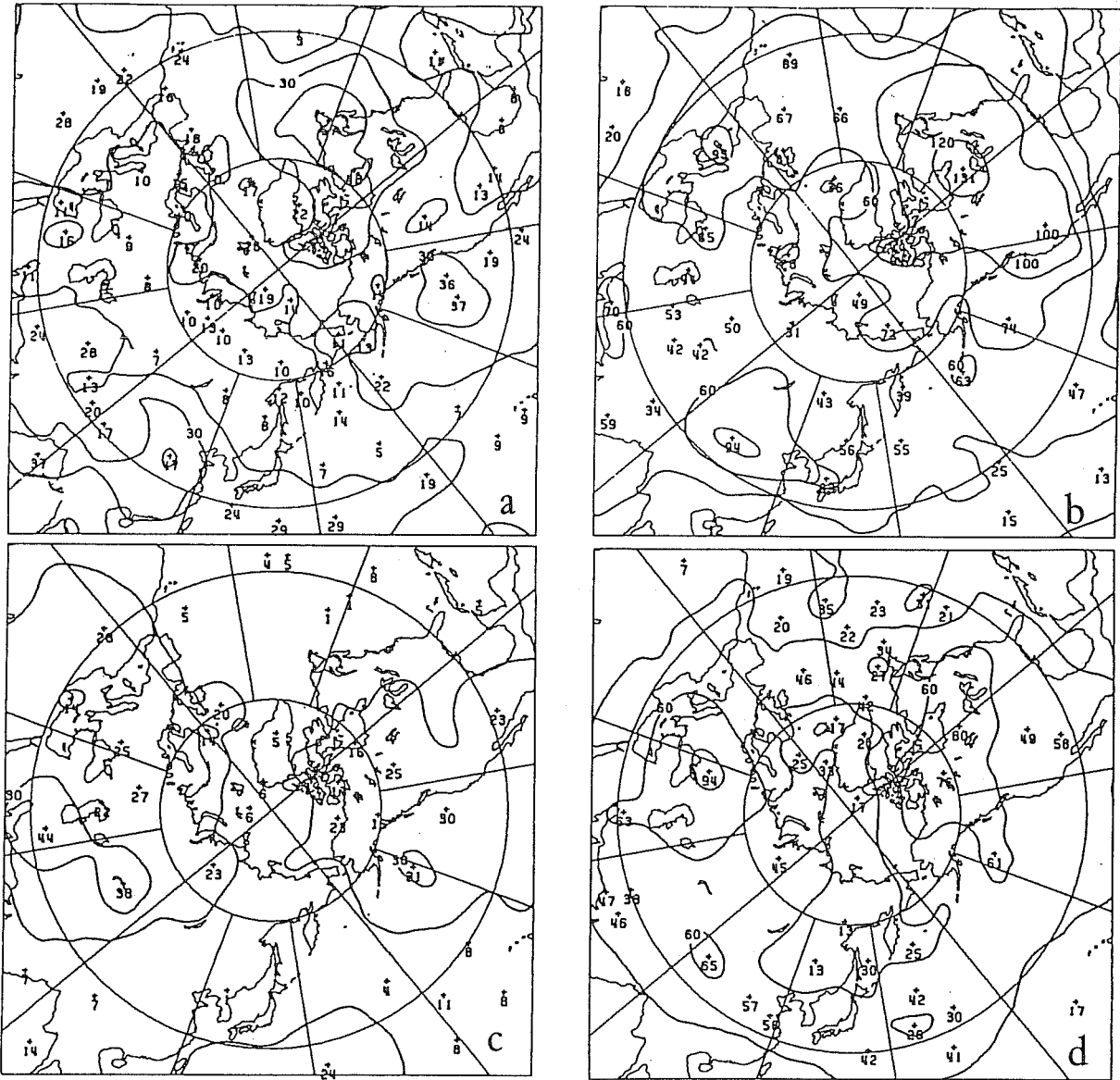
Fig.6   The RMS differences between analysis and guess fields.
(a) CONTL 500mb, (b) CONTL 200mb
(c) SATEL 500mb, (d) SATEL 200mb
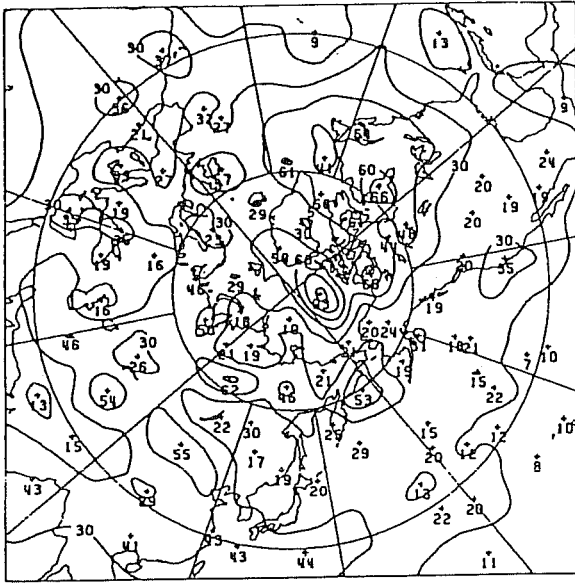
Fig.7 The RMS differences between
       CONTL and SATEL height
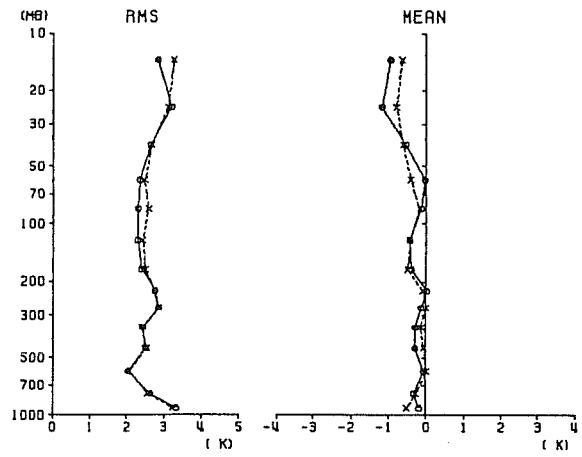   analysis at 500mb.

Fig.8 The RMS and mean differences
       between sonde and SATEM
       thickness temperature
       over northern hemisphere
       for March 1984.
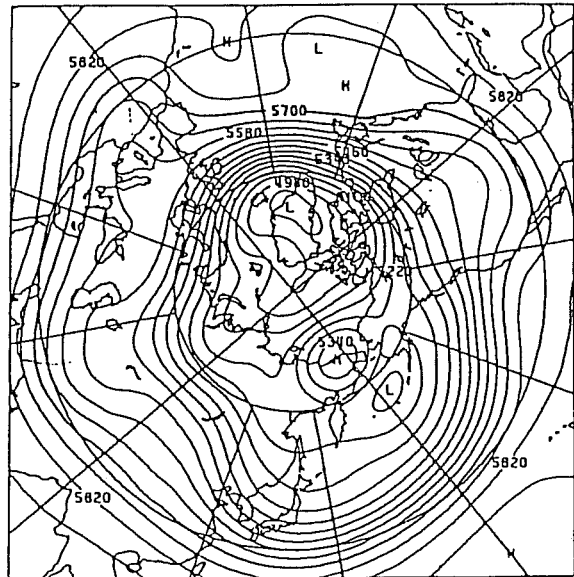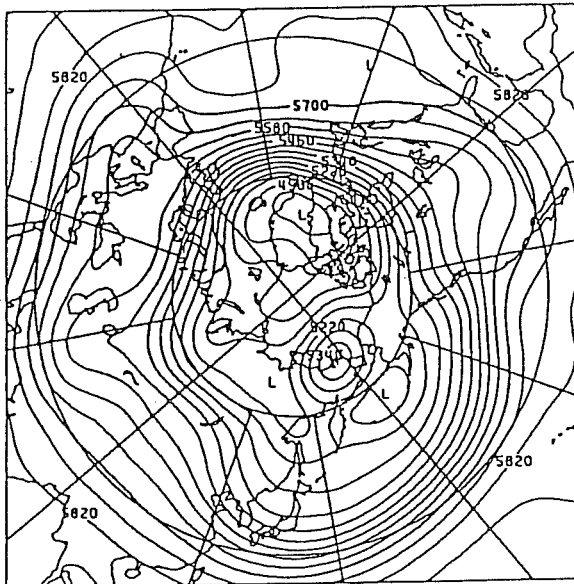   •——• 0-3 hours from map time
       -- 4-6 hours from map time

Fig.9 Mean analyzed height fields over northern hemisphere at 500mb.
       CONTL (left) and SATEL (right)
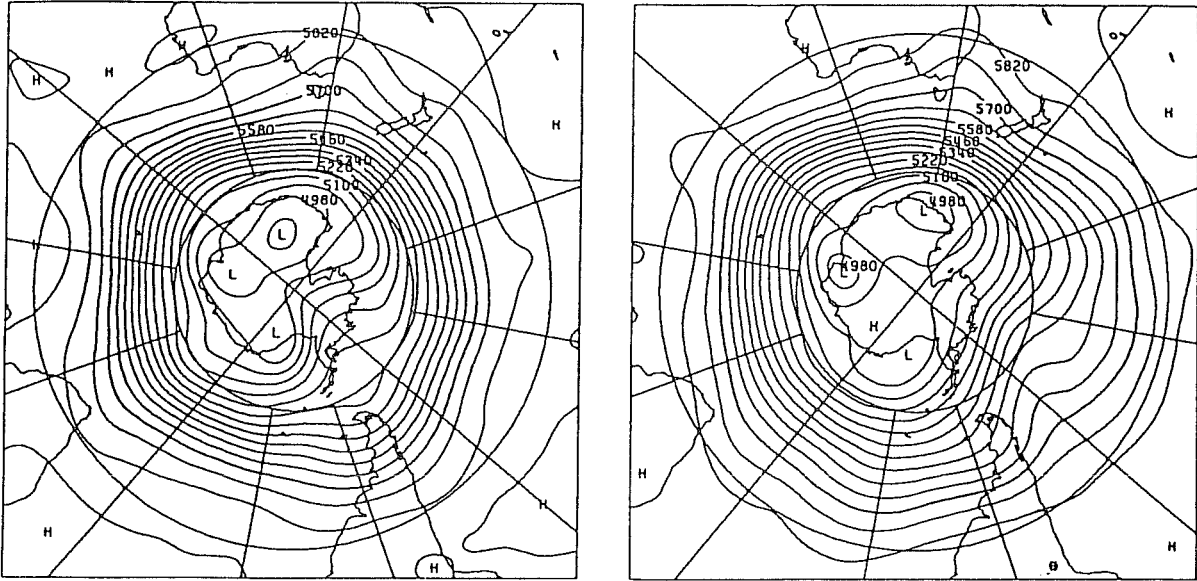
Fig.10 Mean analyzed height fields over southern hemisphere at 500mb.
CONTL (left) and NOSAT (right)
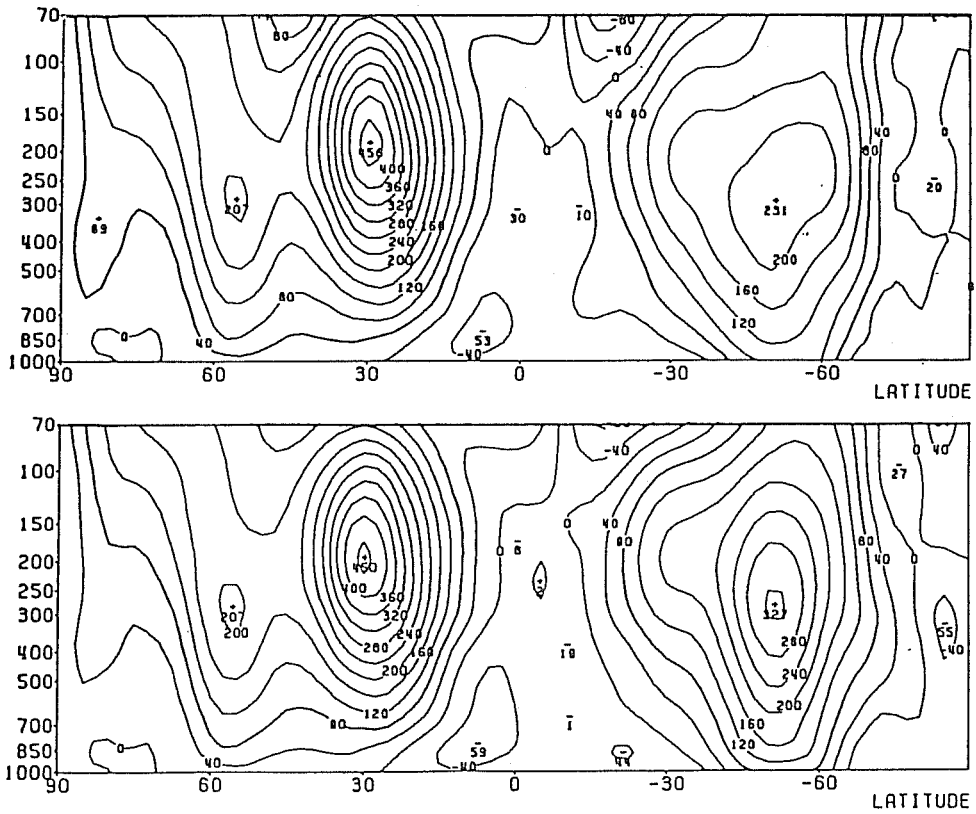
Fig.11 Zonally averaged mean wind fields
for NOSAT (top) and CONTL (bottom).

Labrador peninsula, the inaccurate guess fields are strongly corrected by sonde data in CONTL, but the guess fields remain in SATEL because no data exist. Accordingly, a large difference in the analyses occurs over these areas.

Fig. 8 shows the RMS differences between sonde and SATEM thickness temperatures. The results indicate that observational errors are the same for SATEMs within 0-3 hours of the analysis time, and for SATEMs within 4-6 hours of this time.

Considering the above two facts, we infer that at least for our system when data from only one satellite are available, a 12-hour cycle which utilizes ±6h satellite data over the whole area will give a better analysis than a 6-hour cycle which can utilize ±3h satellite data over only part of the analysis area.

6.2 Middle and high latitudes over the southern hemisphere

In order to get some insight into the analysis accuracy over the southern hemisphere, we first investigate characteristic features of SATEL over the northern hemisphere. Fig. 9 shows the mean 500 mb analysed height over the northern hemisphere for the CONTL and SATEL modes. As far as the mean fields are concerned, the major lows, troughs and ridges are well analysed, even in SATEL.

Fig. 10 depicts the mean 500 mb height analysis over the southern hemisphere. It is seen from Fig. 10 and Table 2 that in this hemisphere the differences between CONTL and NOSAT are very large, except around Australia, South America and the southern part of Africa. NOSAT cannot represent the major synoptic

features; the troughs at 210°E and 330°E and the ridge at 270°E in NOSAT are

not depicted in CONTL. Moreover the baroclinicity is weak, particularly

around 180°-270°E in NOSAT. This is also confirmed by Fig.11 which shows that

the maximum wind speed around the jet core in the zonally-averaged mean wind

field of NOSAT is 30% weaker than that of CONTL (in the case of the northern

hemisphere, the maximum zonal mean wind speed of SATEL is 10% less than that

of CONTL).

The above result indicates that satellite date are essential in the southern

hemisphere.

Also there are large differences between NOSAT and CONTL in the stratospheric

analysis. However, the differences are not confined to specific regions, as

found in the northern hemisphere.

6.3   Tropical area

Fig. 12 shows the streamlines for the mean analysed wind field. At 850 mb,

the field analysed by CONTL is similar to that analysed by NOSAT around

Africa, Saudi Arabia, India, Australia, Caribbean Sea and South America where

sonde and pilot data are relatively dense. In the CONTL analysis,

anticyclonic circulations centred around (30°N,225°E), (30°S 195°E), (27°S,

245°E) and (35°S, 350°E), and systems over the Indian Ocean are depicted by

SATOBs (compare CONTL and SATEL). In NOSAT, the above mentioned anticyclonic

circulations or systems are analysed at different positions or are distorted.

The NOSAT analysis tends to analyse a large number of vortex centres as seen

over the Indian Ocean; these are present in the guess field and therefore

they are generated by the forecast model.

Similar results are often found at other levels. At 200 mb, large scale characteristic features such as the mid-Pacific trough are better analysed than at 850 mb, even in NOSAT. This is because we can utilize AIREPs at 200 mb. However, cross-equatorial winds around 70°E over the Indian Ocean are not well analysed since they are mainly depicted by the SATOBs.

At 300 mb, analyses by CONTL and SATEL are exceptionally similar around South East Asia (10°N-10°S, 90°E-130°E). The wind field at 300 mb in NOSAT is similar to that at 500 mb, while in the CONTL analysis it resembles that at 200 mb. Table 3 shows the RMS differences between analysis and sonde or SATOB. Analyses by CONTL fit sonde data better than those by NOSAT at this level. This shows that SATOBs are very important over regions where sonde data are sparse since they correct the poor quality guess field.

The characteristics found in synoptic fields discussed above are also seen in statistical comparisons. Except at 150 mb the RMS differences between analysis and sonde observations from CONTL are almost the same as those for NOSAT, and they are smaller than the RMS differences between analysis and SATOBs. This indicates that in our analysis system the SATOB and sonde data are properly mixed to yield an analysed wind field according to the observation error given to each data source.

At 150 mb the RMS differences between sonde data and the analysis in CONTL becomes larger than in NOSAT, and they are the same as the RMS difference between SATOBs and the analysis. This suggests that the observation error assigned to SATOBs are too small at this level.
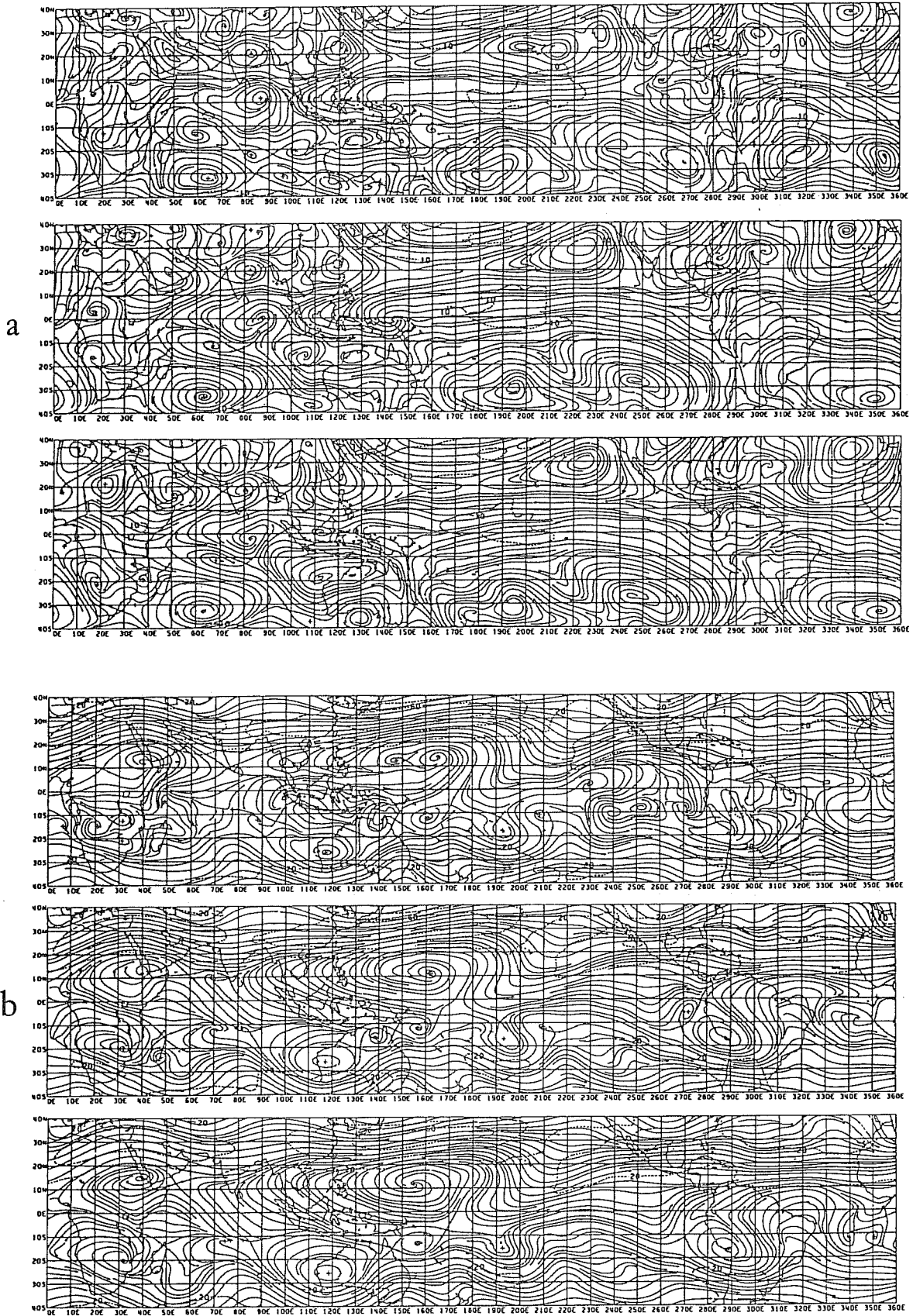
Fig.12   The streamlines for mean analyzed wind field.
         (a) 850mb   NOSAT(top), CONTL(middle), SATEL(bottom)
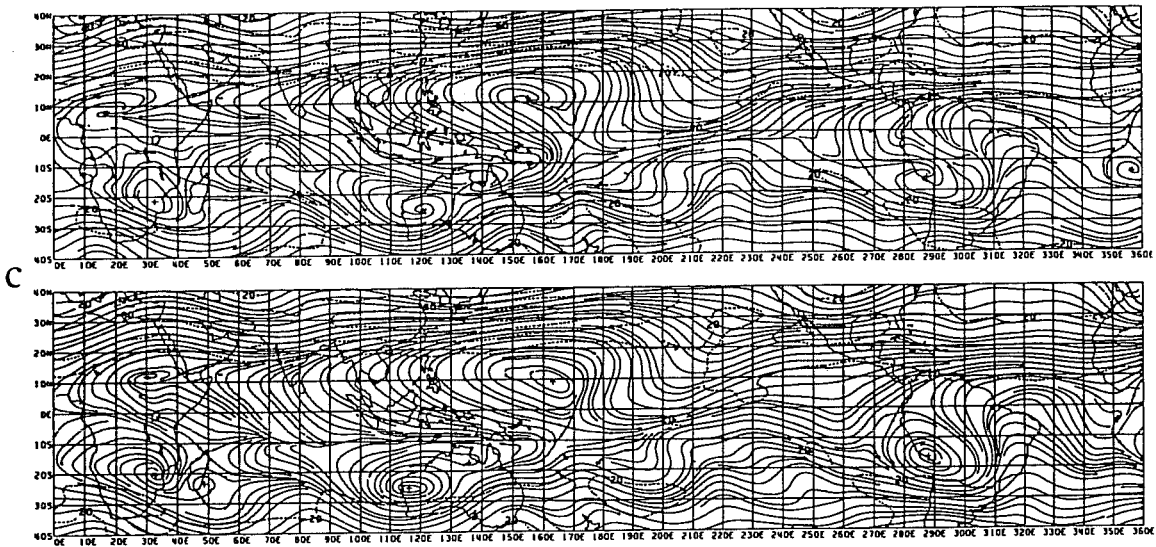   (b) 300mb   NOSAT(top), CONTL(middle), SATEL(bottom)

Fig.12 The streamlines for mean analyzed wind field.
(c) 200mb NOSAT(top), CONTL(bottom)

VARI-ABLE	AREA	MODE	LEVEL(mb)					
			850	500	300	250	200	150
U(m/s)	S.ASIA	NOSAT	2.5	2.9	3.0	3.4	3.6	.4.0
		CONTL	2.3	2.9	2.7	3.1	3.5	3.9
	S.TROP	NOSAT	1.7	3.4	5.2	5.9	6.7	4.0
		CONTL	1.7	3.5	2.9	3.3	4.8	5.6
	SATOB1	CONTL	3.1	–	5.0	4.7	4.4	4.6
	SATOB2	CONTL	2.0	–	5.5	4.6	5.1	5.9
V(m/s)	S.ASIA	NOSAT	2.4	3.3	4.1	4.4	4.2	5.4
		CONTL	2.4	3.2	3.5	4.2	4.4	5.1
	S.TROP	NOSAT	2.5	2.7	3.9	6.8	2.6	2.1
		CONTL	2.5	2.0	2.6	4.2	3.6	4.7
	SATOB1	CONTL	2.6	–	6.4	5.8	4.5	4.9
	SATOB2	CONTL	2.2	–	5.2	4.9	4.6	5.4

Table 3 Averaged RMS of differences between analysis and
sonde (S.ASIA, S.TROP) or SATOB (SATOB1, SATOB2).
Domains of abbreviated areas are as follws.
S.ASIA : 5N-20N, 60E-130E ; S.TROP : 0S-10S, 0E-360E
SATOB1 : 5N-25N, 0E-130E ; SATOB2 : 0S-30S, 90E-180E

255

7.   STATISTICAL EVALUATION OF SATELLITE IMPACT ON THE FORECAST

Tables 4 and 5 show nine-case mean S1 scores and RMS hight errors of the forecasts at 850, 500 and 300 mb. In these tables, DIFF indicates (NOSAT-CONTL) and a positive value of DIFF implies a positive impact of satellite data on the forecasts. The overall statistical verification of forecasts against analyses is summarized in these tables. The CONTL analyses are used as verification fields, but verification scores depend on the choice of verifying analysis. However, in data-rich areas such as East Asia, North America and Europe the choice of verifying analyses does not make much difference because of the very small difference between NOSAT and CONTL analyses (see Sect.6).

It is clear from these tables that there is almost no difference between the forecasts generated from NOSAT and CONTL analyses over East Asia and Europe. On the other hand, over North America forecasts from CONTL analyses are clearly better than forecasts from NOSAT analyses.

Tables 6 and 7 show daily S1 scores and the RMS height error of forecasts at 500 mb over East Asia and North America. Over North America, the verification scores show the positive impact of satellite data, except for two cases in the 72-hour RMS values. Furthermore, these scores do not strongly depend on the large biases over the Pacific region mentioned in Sect.6. For example, the S1 scores for the 48-hour forecasts from the analyses for 27 and 28 February which have small biases are worse than those from 6 and 7 March which have large biases. Over East Asia, both negative and positive impacts appear. The confidence limits applied to the 9-case mean, which are based on the Student's t 95% values, are shown after the mean values in Table 6 and 7. These values indicate that the mean positive impact on the forecasts over North America is statistically significant, however this is not so for the mean impact over East Asia.

Because the differences between NOSAT and CONTL analyses over the upstream region of East Asia are very small, the null impact of satellite data on these areas is not surprising. On the other hand, the positive impact in North America is gained by the improvement in the analyses over the upstream Pacific region.

Verification scores of forecasts from NOSAT are considerably lower over the southern hemisphere, even for 24-hour forecasts. The magnitude of the score varies little with forecast time. This indicates that NOSAT analyses themselves, which are generated by the assimilation system with almost no data, have no significant value.

In the tropics, the RMS errors of both modes are very small in accordance with the small natural variance, but the S1 scores for both modes are worse than in the other regions because of the small gradients in the tropics.

850MB

TIME (hr)	MODE	AREA						
		E.ASIA	PACIFC	N.AMER	ATLANT	EUROPE	S.HEM	TROPIC
	NOSAT	60.6	50.0	55.5	37.2	45.2	67.5	80.7
48	CONTL	61.6	46.3	52.2	37.2	43.5	54.7	76.0
	DIFF	-1.6	3.7	3.3	0.1	1.7	12.8	4.7
	NOSAT	70.2	57.1	65.5	41.9	50.7	70.3	81.9
72	CONTL	72.1	53.7	58.5	43.0	51.3	59.9	78.4
	DIFF	-1.9	3.4	7.0	-1.1	-0.7	10.5	3.5

500MB

TIME (hr)	MODE	AREA						
		E.ASIA	PACIFC	N.AMER	ATLANT	EUROPE	S.HEM	TROPIC
	NOSAT	22.0	32.7	27.9	25.3	27.6	59.8	67.1
24	CONTL	21.7	23.8	22.9	22.2	27.5	34.8	59.6
	DIFF	0.3	8.9	5.0	3.1	0.1	25.0	7.5
	NOSAT	31.6	37.1	40.2	30.2	38.9	64.2	70.7
48	CONTL	31.7	32.8	34.4	28.8	37.2	47.8	66.2
	DIFF	-0.0	4.3	5.8	1.4	1.7	16.3	4.5
	NOSAT	37.8	41.6	49.9	34.8	48.1	66.7	72.0
72	CONTL	38.6	39.4	42.5	34.5	48.2	54.6	68.3
	DIFF	-0.8	2.2	7.4	0.4	-0.1	12.1	3.7
	NOSAT	42.7	48.9	57.8	41.9	52.5	67.6	74.0
96	CONTL	44.3	47.3	51.1	37.1	55.2	59.5	70.8
	DIFF	-1.6	1.7	6.7	4.9	-2.7	8.1	3.2

300MB

TIME (hr)	MODE	AREA						
		E.ASIA	PACIFC	N.AMER	ATLANT	EUROPE	S.HEM	TROPIC
	NOSAT	28.5	35.9	41.2	32.1	37.0	61.6	62.9
48	CONTL	28.2	31.1	32.3	30.9	35.3	44.3	57.4
	DIFF	0.3	4.8	8.9	1.3	1.7	17.3	5.5
	NOSAT	33.1	39.5	49.7	34.7	48.3	63.8	64.9
72	CONTL	33.5	37.3	42.1	34.0	47.2	51.7	61.1
	DIFF	-0.5	2.3'	7.6	0.7	1.2	12.0	3.8

Table 4 Nine-case mean S1 scores over various areas for
         height forecast at 850, 500 and 300mb levels.
                  DIFF=NOSAT-CONTL
         Domains of abbreviated areas are as follws.
     E.ASIA : 25N-60N,   90E-150E   ;   PACIFC : 25N-60N, 150E-230E
     N.AMER : 25N-60N, 230E-300E   ;   ATLANT : 25N-60N, 300E-350E
     EUROPE : 30N-70N,   10W- 50E   ;   S.HEM : 20S-90S,   0E-360E
     TROPIC : 25N-25S,   0E-360E

850MB

TIME (hr)	MODE	AREA						
		E.ASIA	PACIFC	N.AMER	ATLANT	EUROPE	S.HEM	TROPIC
48	NOSAT	42.4	54.2	38.1	27.3	37.9	71.7	17.8
	CONTL	44.3	49.9	36.0	28.2	36.2	49.8	18.1
	DIFF	-1.8	4.3	2.0	-0.8	1.7	21.9	-0.3
72	NOSAT	52.6	67.6	50.8	36.1	53.6	75.9	20.8
	CONTL	52.1	62.5	46.4	39.1	55.5	56.7	18.7
	DIFF	0.5	5.2	4.4	-3.0	-1.9	19.2	2.2

500MB

TIME (hr)	MODE	AREA						
		E.ASIA	PACIFC	N.AMER	ATLANT	EUROPE	S.HEM	TROPIC
24	NOSAT	21.0	59.5	33.0	31.2	30.8	102.7	22.8
	CONTL	19.3	33.2	26.0	24.6	30.0	46.6	19.1
	DIFF	1.7	26.3	7.0	6.6	0.8	56.1	3.7
48	NOSAT	37.4	66.9	52.5	37.6	55.4	110.6	23.8
	CONTL	35.3	51.7	41.3	37.4	54.2	67.7	20.1
	DIFF	2.2	15.2	11.2	0.2	1.2	42.9	3.7
72	NOSAT	45.5	79.5	73.5	50.0	79.7	115.4	26.4
	CONTL	44.0	71.6	61.7	50.0	78.2	83.5	21.7
	DIFF	1.4	7.9	11.8	-0.0	1.4	31.8	4.8
96	NOSAT	58.0	110.8	95.3	57.4	95.2	116.8	28.3
	CONTL	61.8	95.1	83.3	59.5	93.7	92.2	23.9
	DIFF	-3.8	15.6	11.9	-2.1	1.5	24.6	4.4

300MB

TIME (hr)	MODE	AREA						
		E.ASIA	PACIFC	N.AMER	ATLANT	EUROPE	S.HEM	TROPIC
48	NOSAT	50.4	80.2	78.7	53.7	69.4	148.7	34.1
	CONTL	45.8	57.4	56.5	55.5	70.9	83.8	27.7
	DIFF	4.6	22.8	22.2	-1.8	-1.5	65.0	6.3
72	NOSAT	60.1	94.1	102.3	67.6	102.6	153.5	38.2
	CONTL	60.8	85.6	84.2	66.7	100.5	105.4	32.5
	DIFF	-0.7	8.5	18.1	0.9	2.1	48.1	5.8

Table 5　The same as Table 4 except for RMS height errors.

```
                              E.ASIA
TIME    MODE                    DATE                              MEAN
(hr)           2/27  2/28  3/1   3/2   3/3   3/4   3/5   3/6   3/7

        NOSAT  33.8  31.5  29.4  34.2  29.6  31.4  27.7  33.2  34.0   31.6
  48    CONTL  34.1  28.1  29.7  34.2  31.5  32.6  27.9  33.4  33.5   31.7
        DIFF   -0.3   3.4  -0.3  -0.0  -1.9  -1.2  -0.3  -0.1   0.5  -0.0±1.12

        NOSAT  40.4  35.8  38.0  37.9  35.5  36.4  32.3  37.3  46.4   37.8
  72    CONTL  42.0  38.1  39.8  37.7  33.4  36.5  33.9  40.7  45.1   38.6
        DIFF   -1.5  -2.3  -1.9   0.2   2.1  -0.1  -1.6  -3.3   1.3  -0.8±1.36


                              N.AMER
TIME    MODE                    DATE                              MEAN
(hr)           2/27  2/28  3/1   3/2   3/3   3/4   3/5   3/6   3/7

        NOSAT  41.8  46.4  31.0  36.8  43.9  41.7  41.6  38.5  39.8   40.2
  48    CONTL  40.7  33.5  28.8  27.8  37.5  35.6  36.5  32.0  37.1   34.4
        DIFF    1.0  12.9   2.2   9.0   6.4   6.2   5.1   6.5   2.7    5.8±2.82

        NOSAT  52.1  43.2  43.4  54.0  48.3  46.0  47.8  59.6  54.5   49.9
  72    CONTL  48.8  38.6  34.5  35.8  45.7  42.8  42.3  48.0  45.9   42.5
        DIFF    3.3   4.6   8.9  18.2   2.6   3.3   5.6  11.6   8.6    7.4±3.91
```

Table 6   Daily S1 scores over East Asia and North America
for 48 and 72hr height forecasts at 500mb.
(DIFF=NOSAT-CONTL)

```
                              E.ASIA
TIME    MODE                    DATE                              MEAN
(hr)           2/27  2/28  3/1   3/2   3/3   3/4   3/5   3/6   3/7

        NOSAT  31.2  32.7  28.2  39.8  40.8  39.2  39.9  35.2  49.8   37.4
  48    CONTL  32.6  29.1  27.5  37.7  36.0  36.6  40.9  37.1  39.9   35.3
        DIFF   -1.4   3.6   0.7   2.1   4.8   2.7  -1.0  -1.9   9.9    2.2±2.86

        NOSAT  42.7  31.0  44.9  45.3  45.4  51.0  42.3  48.5  57.9   45.5
  72    CONTL  45.9  32.8  41.3  38.8  39.2  51.9  46.2  51.2  49.1   44.0
        DIFF   -3.2  -1.8   3.6   6.5   6.2  -0.8  -3.9  -2.7   8.9    1.4±3.76


                              N.AMER
TIME    MODE                    DATE                              MEAN
(hr)           2/27  2/28  3/1   3/2   3/3   3/4   3/5   3/6   3/7

        NOSAT  45.3  65.1  44.1  46.2  55.5  54.7  63.1  44.5  54.2   52.5
  48    CONTL  42.4  43.4  32.6  32.9  43.5  40.8  55.2  39.1  41.9   41.3
        DIFF    2.9  21.7  11.5  13.3  12.0  13.9   7.9   5.4  12.3   11.2±4.19

        NOSAT  78.3  85.5  59.3  72.8  59.9  71.4  60.1  89.9  84.5   73.5
  72    CONTL  63.9  62.1  54.6  51.9  66.0  61.6  70.4  59.9  64.7   61.7
        DIFF   14.4  23.3   4.7  21.0  -6.1   9.8 -10.3  30.0  19.7   11.8±10.5
```

Table 7   The same as Table 6 except for RMS height errors.

8.   CASE STUDY

Fig. 13(a), (b) shows the 500 mb geopotential height at 00GMT 1 March analysed by CONTL and NOSAT, and the differences between these is exhibited in Fig. 17(c). In the CONTL analysis the ridge around 210°E and the deep trough to the west of North America are more intense than in NOSAT. Accordingly the height gradient between the above mentioned ridge and trough is strong in CONTL; the maximum height difference over this area is +152 m. Moreover, the ridge extending from south of Aleutian to Sakhalin and the trough to the east of this ridge are analysed differently in CONTL and NOSAT. Fig. 14 shows the thickness temperature between 1000 mb and 500 mb at 00GMT 1 March. In CONTL there is a warm core around (40°N, 210°E), while in NOSAT there are weak thermal troughs extending into this area. The temperature gradient to the west of North America is very weak in NOSAT compared to that in CONTL.

A significant difference between CONTL and NOSAT is the maximum centred around (40°N, 215°E). We now discuss how this difference is generated by tracing the 500 mb height difference (hereafter denoted by Δz; Δz = CONTL-NOSAT) through each analysis time for both analysed and guess values.

Fig. 15(a) shows Δz and the CONTL analysis at 18GMT 27 February. The ridge around (45°N, 195°E) and the Δz maximum of +20 m in its vicinity are now discussed. Fig. 15(b) shows Δz and the guess field which is the 6-hour forecast based on the analysis at 18GMT on the 27th for CONTL. The positive Δz area shifts slightly eastwards and its magnitude increases to 48 m during the forecast. Fig. 15(c) shows the CONTL analysis and Δz at 00GMT 28th, and Fig. 15(d) the data distribution. Although the area of positive Δz becomes large, the magnitude does not change by the utilization of SATEM data. The magnitude of the negative Δz area nearby the positive one decreases with the

introduction of SATEM data. Near California the magnitude of the negative Δz area is reduced by about 50% by sonde data, as the positive area near the Aleutians.

Fig. 16(a) shows the data distribution at 06GMT on the 28th, and Fig. 16(b) the 6-hour forecast starting from the analysis at 06GMT 28th and Δz. Because there are few data to the east of 180°E over the North Pacific at 06GMT, changes in the fields between Fig. 15(c) and Fig. 16(b) are caused by the forecast model. The positive Δz area moves about 10 degrees to the east and the area of positive Δz values is reduced with no change of magnitude. Fig. 16(c) shows the CONTL analysis and Δz at 12GMT 28th and (d) the data distribution, whilst Fig. 18(a),(b) shows corrections to guess values at 12GMT on the 28th for CONTL and NOSAT, respectively. The ridge is intensified and the maximum of positive Δz reaches 83 m. However, the position of the positive Δz does not change. In the NOSAT analysis, guess values near California and Aleutian are modified by sonde data more than in the CONTL analysis, and Δz in the area decreases.

Fig. 17(a) shows the CONTL analysis and Δz at 18GMT on the 28th; the positive Δz does not change its magnitude, but it does move about 10 degrees to the east. The Δz of the guess at 00GMT 1 March is given in Fig. 17(b). Although the positive area does not move, the magnitude increases by 27 m to 111 m. Since there is no data over the Pacific to the east of 180°E, the changes are produced by the forecast model. Fig. 17(c), (d) shows the CONTL analysis, Δz and data distribution at 00GMT 1 March and in Fig. 18(c),(d) are the correction to guess values for both the analysis modes. The positive Δz area is enlarged through the correction by the SATEMs, as happened at 12GMT on the 28th, and the maximum of the positive Δz becomes 152 m (an increase of 41 m).
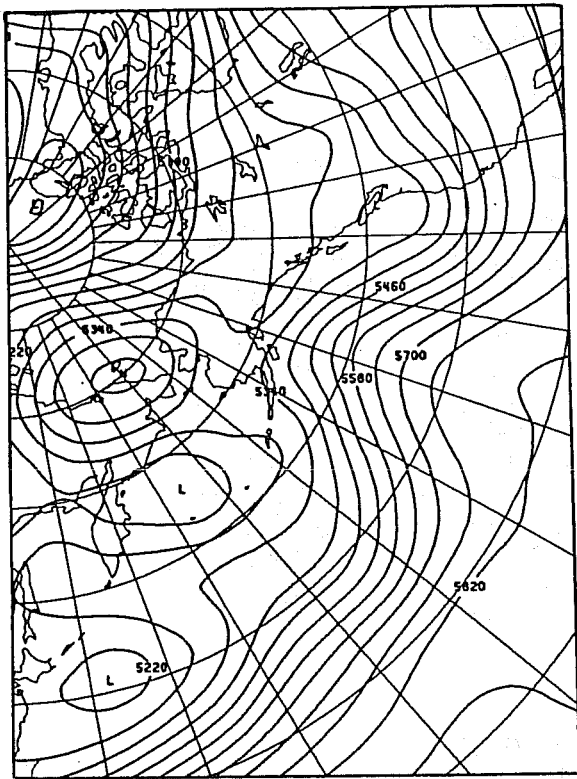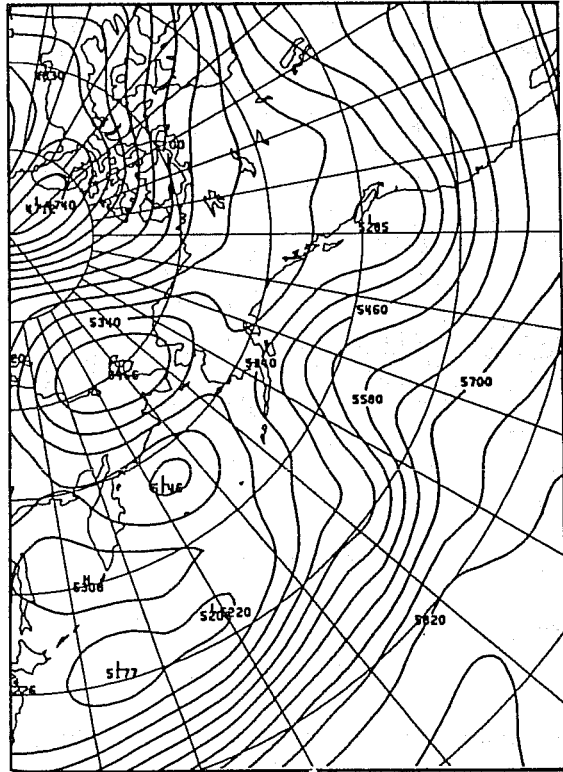
Fig.13 500mb height analyses for 00GMT 1 March 1979.
CONTL (left) and NOSAT (right)
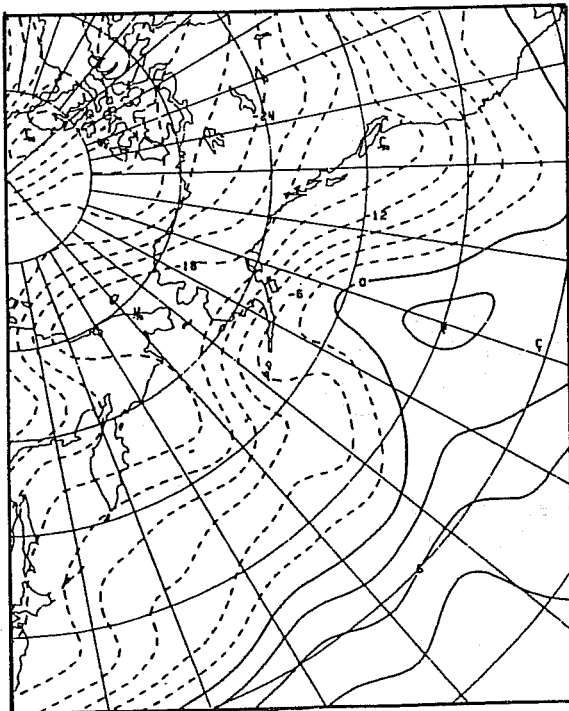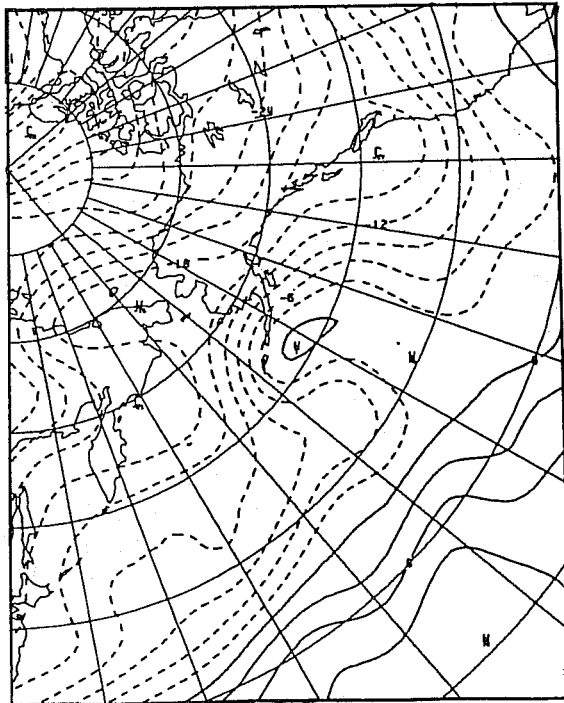
Fig.14 1000-500mb thickness temperature(°C) for 00GMT 1 March.
CONTL (left) and NOSAT (right)
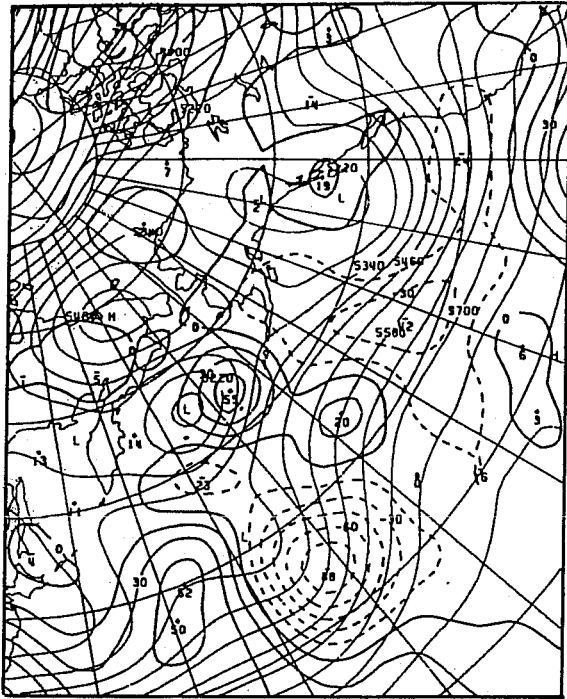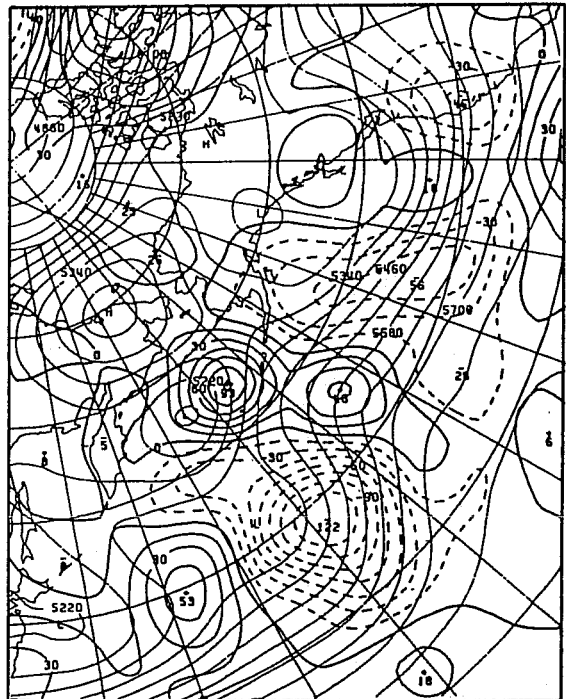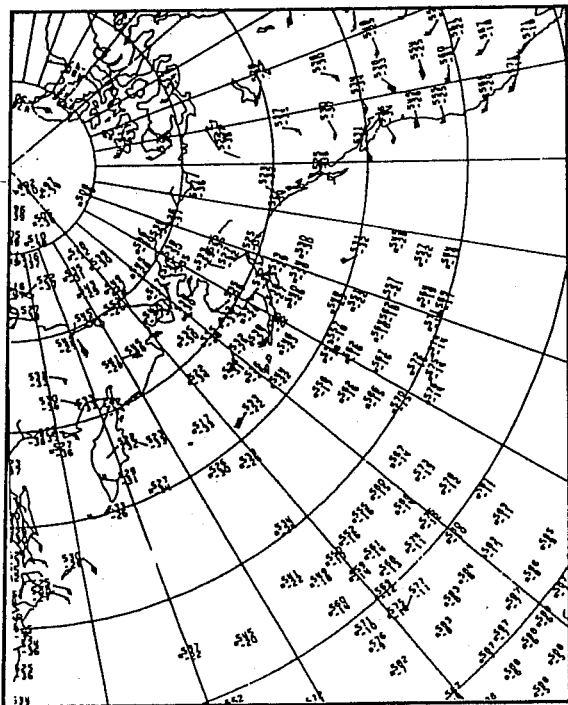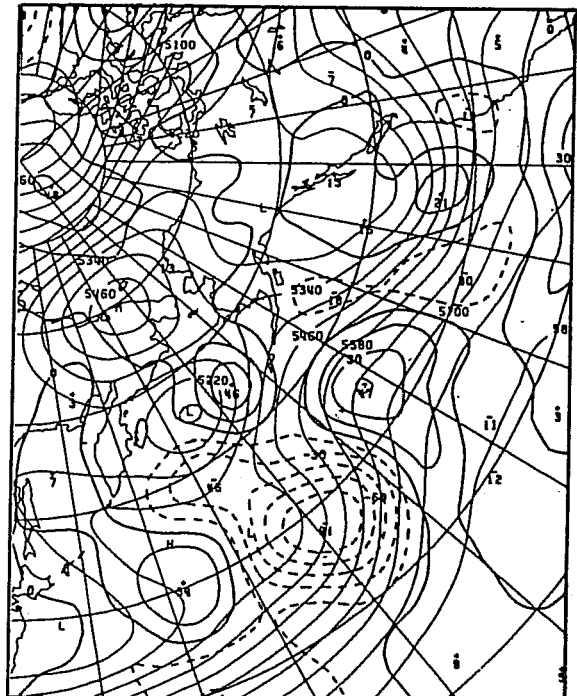
Fig.15 500mb height differences (thick lines, CONTL-NOSAT) and
CONTL 500mb height (thin lines) and data distribution.
          (a) Analysis at 18GMT 27 February
          (b) Guess   at 00GMT 28 February
          (c) Analysis at 00GMT 28 February
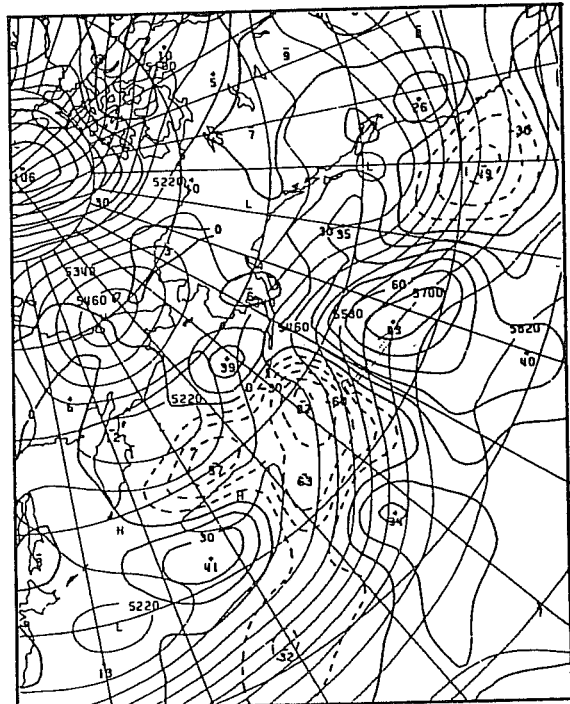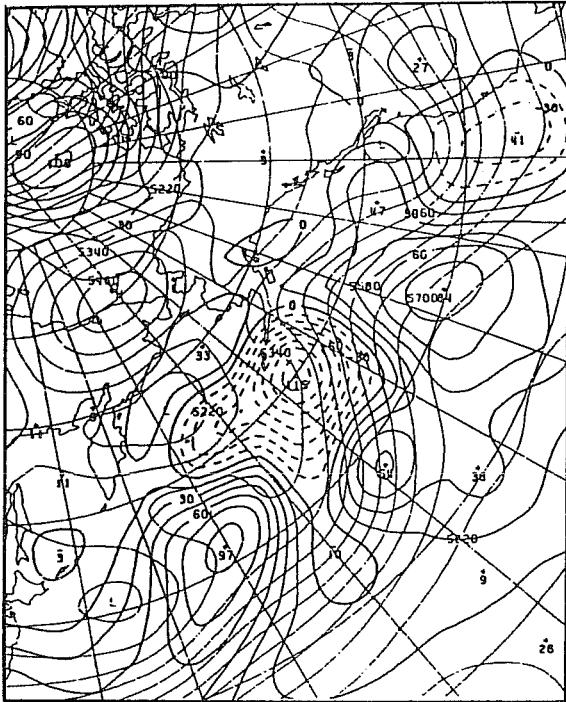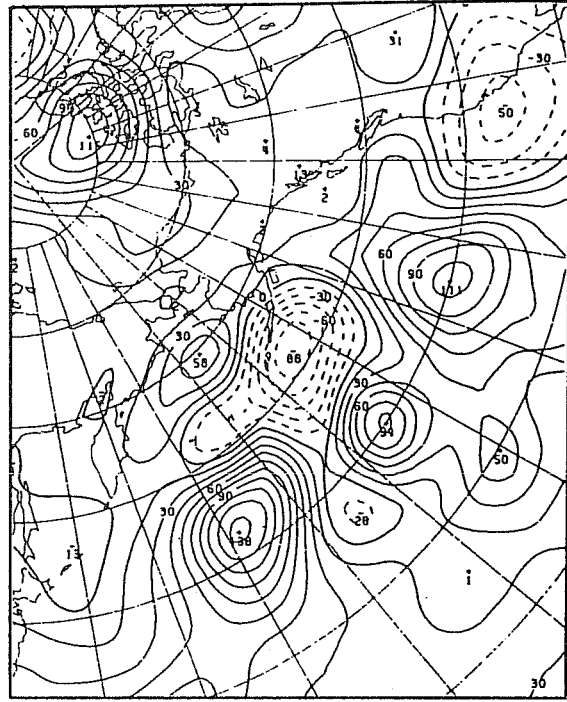   (d) Data   at 00GMT 28 February (✳ : SATEMs)

a

b

d
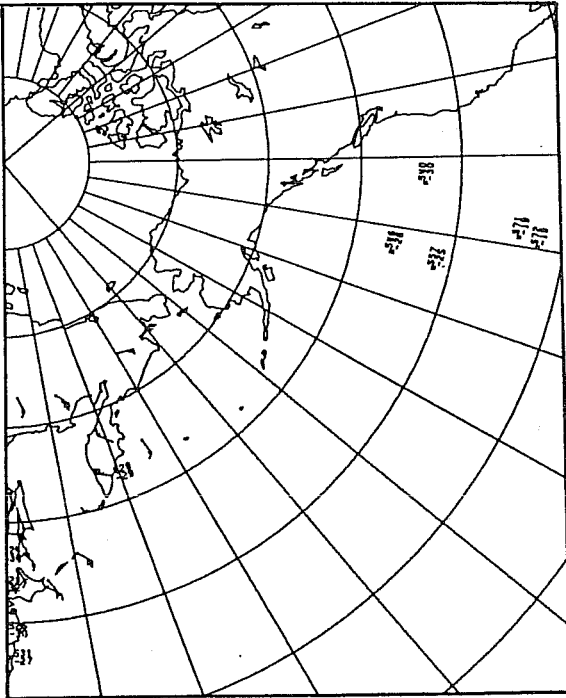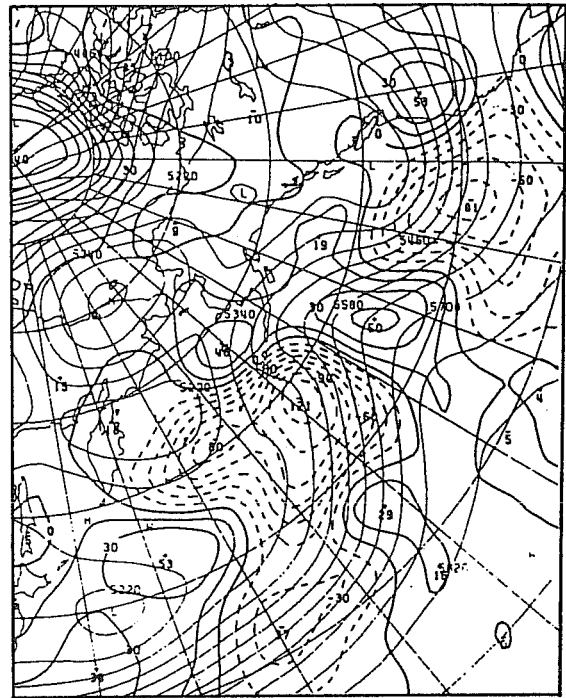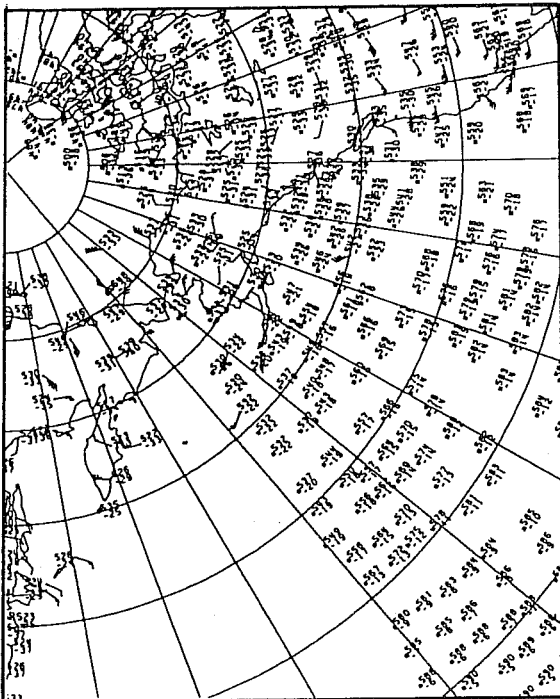
c

Fig.16 The same as Fig.15 except
(a) Data   at 06GMT 28 February (✳ : SATEMs)
(b) Guess   at 12GMT 28 February
(c) Analysis at 12GMT 28 February
(d) Data   at 12GMT 28 February (✳ : SATEMs)
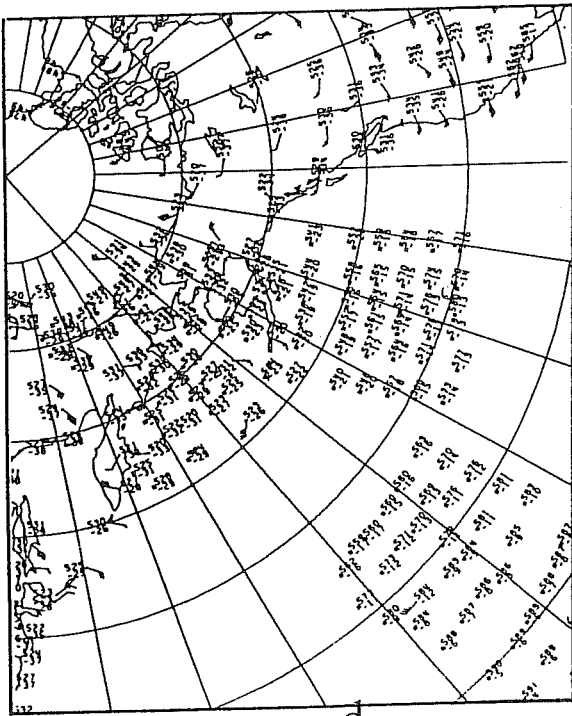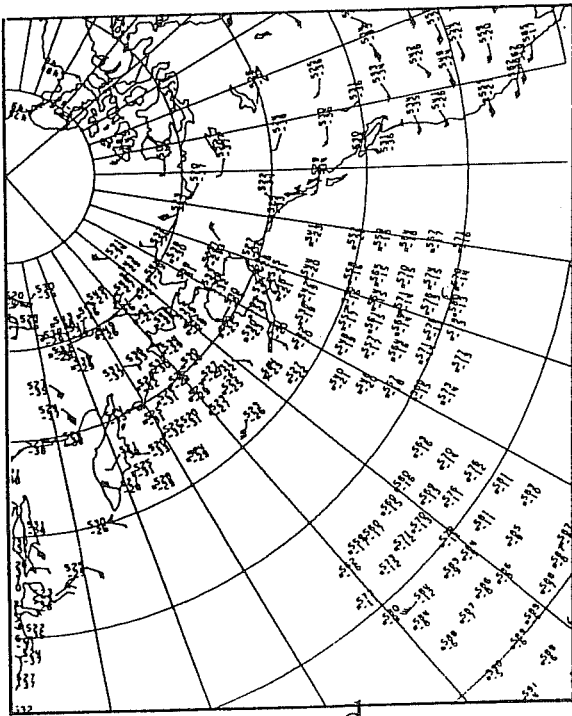
Fig.17 The same as Fig.15 except
        (a) Analysis at 18GMT 28 March
        (b) Guess   at 00GMT 1 March
        (c) Analysis at 00GMT 1 March
        (d) Data   at 00GMT 1 March (＊ : SATEMs)
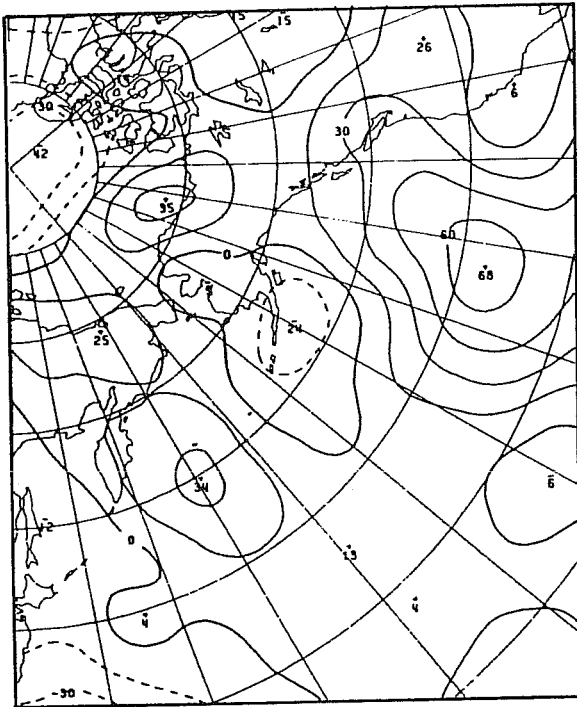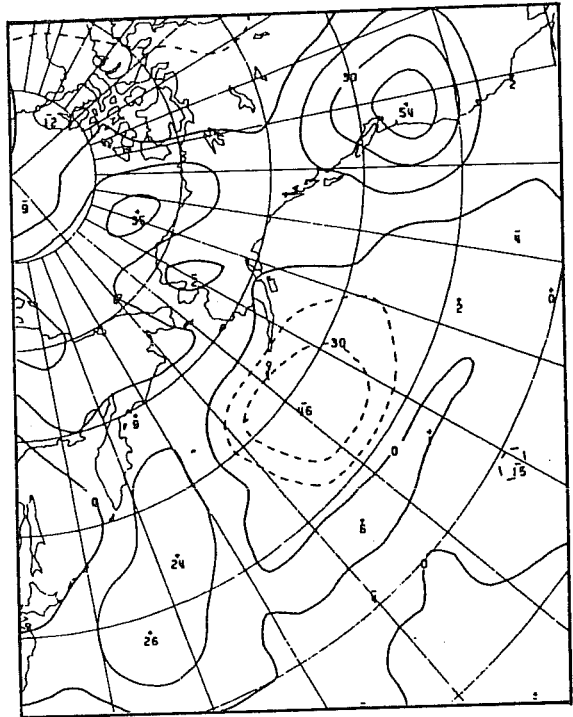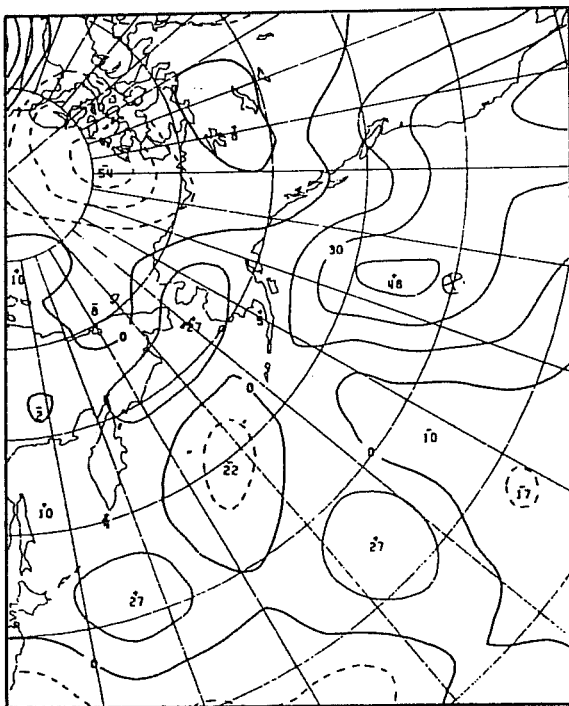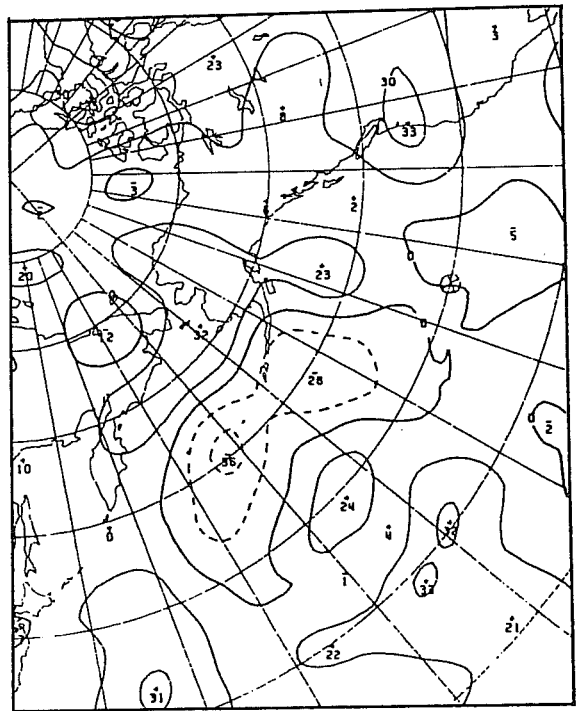
Fig.18　Corrections to 500mb height guess values.
(a) CONTL, (b) NOSAT at 12GMT 28 February
(c) CONTL, (d) NOSAT at 00GMT 1 March

The above results indicate that the difference between analyses at a certain time level are produced not only by the impact of data utilized at that time level but also by the accumulated effect maintained and modified through the assimilation cycle.

Whatever processes are responsible for the generation of analysis differences over the ocean, they are caused by whether or not satellite data are utilised. Therefore, to a considerable extent, the quality of the analysis depends on the quality of satellite data. The accuracy of satellite data at the present time are less than that of sonde data and are almost the same as the accuracy of forecasts. Therefore the existence of the analysis differences caused by the satellite data does not necessarily imply that the quality of the CONTL analysis is better than that of NOSAT. In order to assess the quality of the analyses and to investigate how the differences in analyses influence the forecasts, we compare synoptically the forecasts from the CONTL and NOSAT analyses with the verifying CONTL analysis over North America where sonde data are plentiful and differences between analyses are small.

Figs. 19 and 21 show the 500 mb height forecast from 00GMT 1 March; in these figures (a) is the CONTL forecast, (b) the verifying analysis (CONTL) and (c) the NOSAT forecast. Figs. 20 and 22 show the CONTL-NOSAT forecast differences.

At the initial time large differences are seen near the ridge at 210°E. These decrease during the 24-hour forecast and the position of large difference shifts to the trough region around 240°E where its value is -130 m. In the 48-hour forecast, the area of large difference shifts further east to the Great Lakes where a ridge is analysed. The trough in the 24-hour forecast

and the ridge in the 48-hour forecast are more intense in the CONTL forecast than in NOSAT. The CONTL forecast agrees better with the analysis than the NOSAT forecast.

A trough is analysed at (50°N, 250°E) in CONTL and NOSAT at initial time, and in both 72 hour forecasts it moves to the Labrador Peninsula. However, because the degree of deepening and the position are different, a large negative deviation is found ahead of the positive deviation at the ridge. The negative difference accompanying the trough is further amplified as the forecast progresses and it is found around 340°E in the 120-hour forecast. Examination of Fig. 23, the forecast sea level pressure at 120-hour, shows that NOSAT does not predict the low around (60°N, 335°E) which is predicted by CONTL and verified by the analysis.

Fig. 24 depicts the 500 mb height field predicted at 48 hour (upper) and at 96 hour (lower) from the analysis at 00GMT 28 February. The difference between the two initial analyses in the vicinity of the trough at 225°E (see Fig. 15(c)) amplifies while the trough moves to 240°E and the difference becomes -120 m; a positive difference (+ 150 m) is found in front of the trough. The 48 hour CONTL forecast agrees well with the analysis. After 48 hours, the difference between the two forecasts decreases and forecast quality of both gradually degenerates. There is no noticeable difference between CONTL and NOSAT forecast at 96 hours.

The result of the case studies discussed above, together with the statistical evaluations shown in Tables 6 and 7, indicates that the CONTL analysis yields a better forecast than that from the NOSAT analysis. In other words, the quality of the CONTL analysis is better than that of NOSAT.
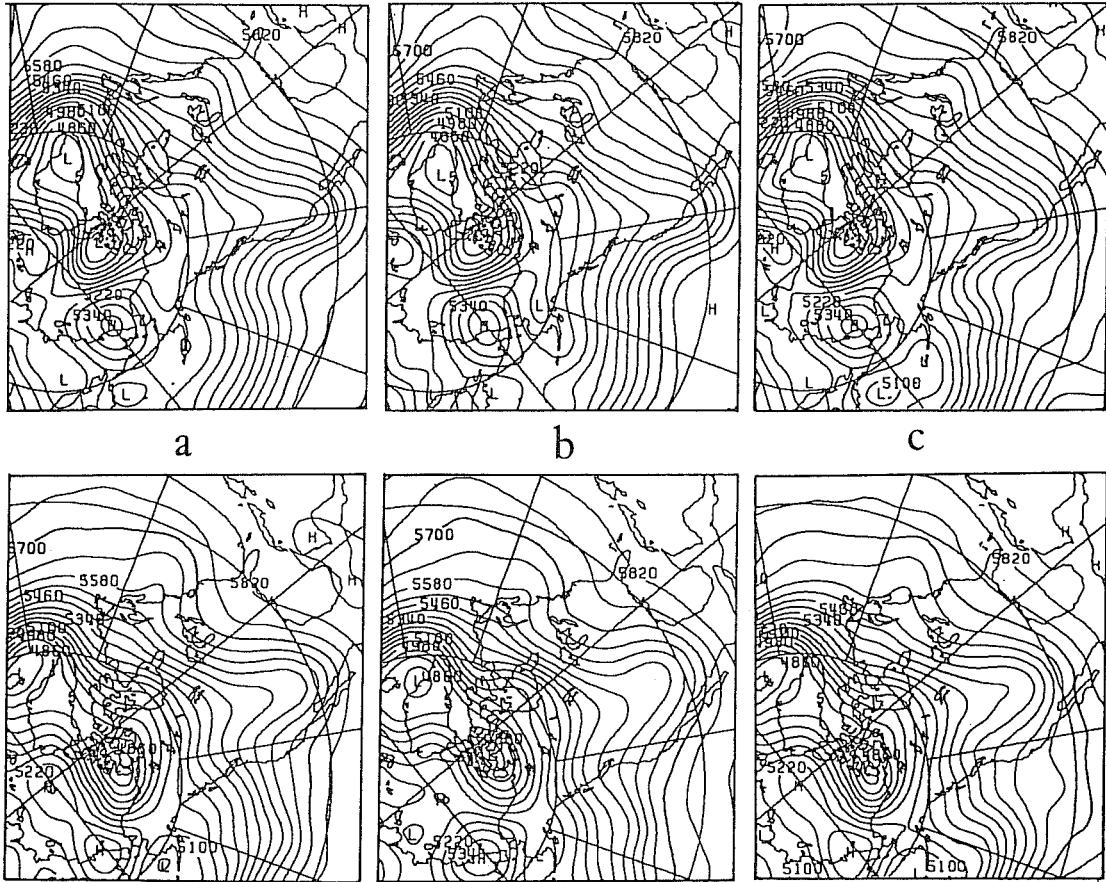
Fig.19　500mb height forecast (CONTL (a), NOSAT (c)) on the basis of
analysis at 00GMT 1 March and verification (b).
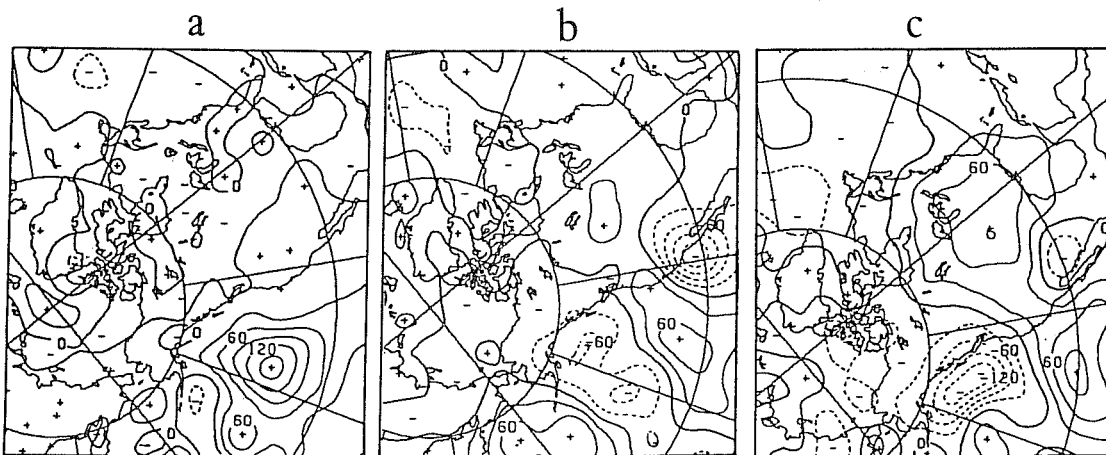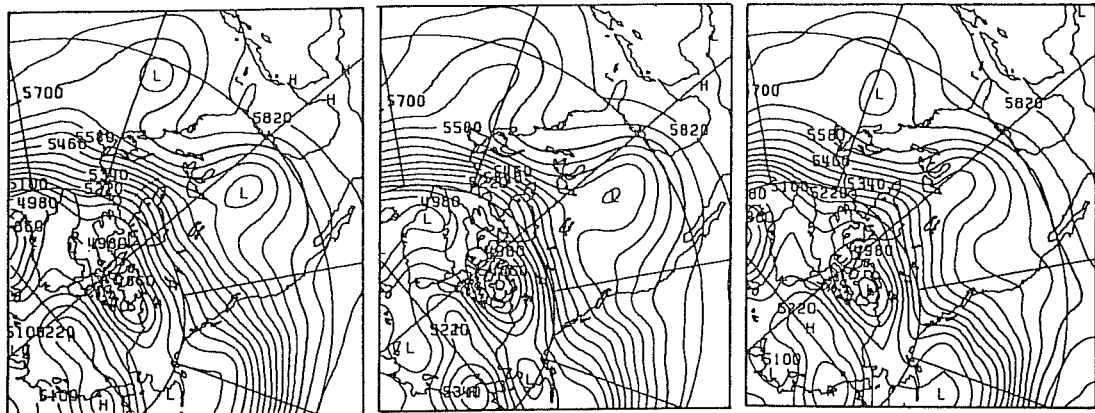top (24 hours), bottom (48 hours)

Fig.20　Difference of 500mb height forecast (CONTL-NOSAT)
from 00GMT 1 March. (a)initial, (b) 24hr, (c) 48hr

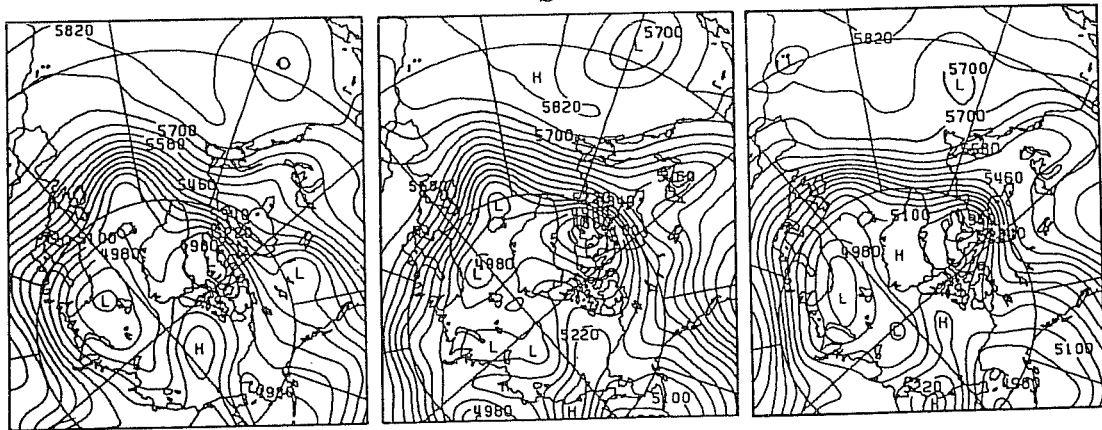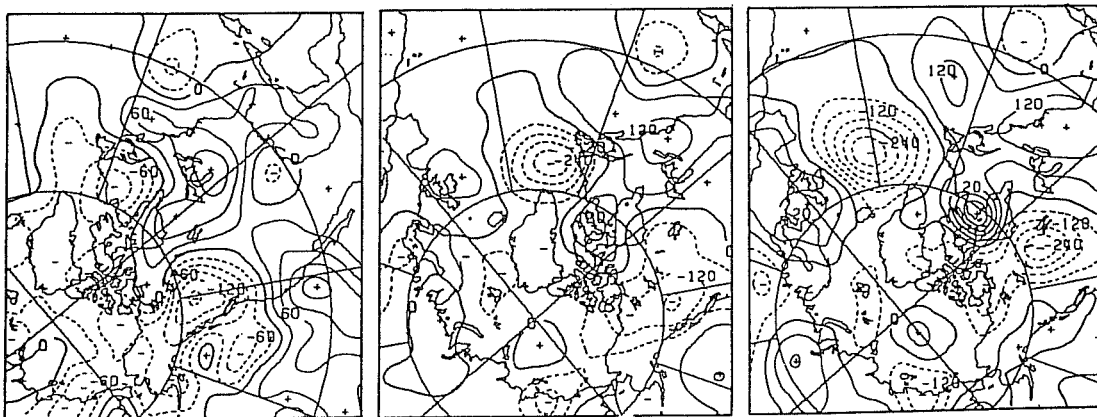Fig.21   The same as Fig.19 except 72hr(top) and 120hr(bottom).

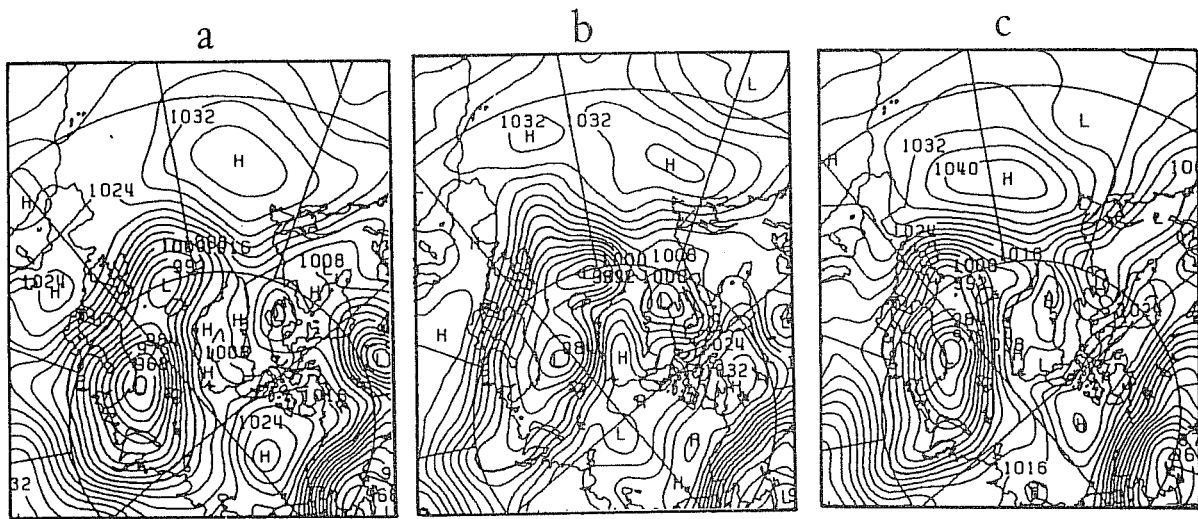fig.22   The same as Fig.20 except (a) 72hr, (b) 96hr, (c) 120hr.

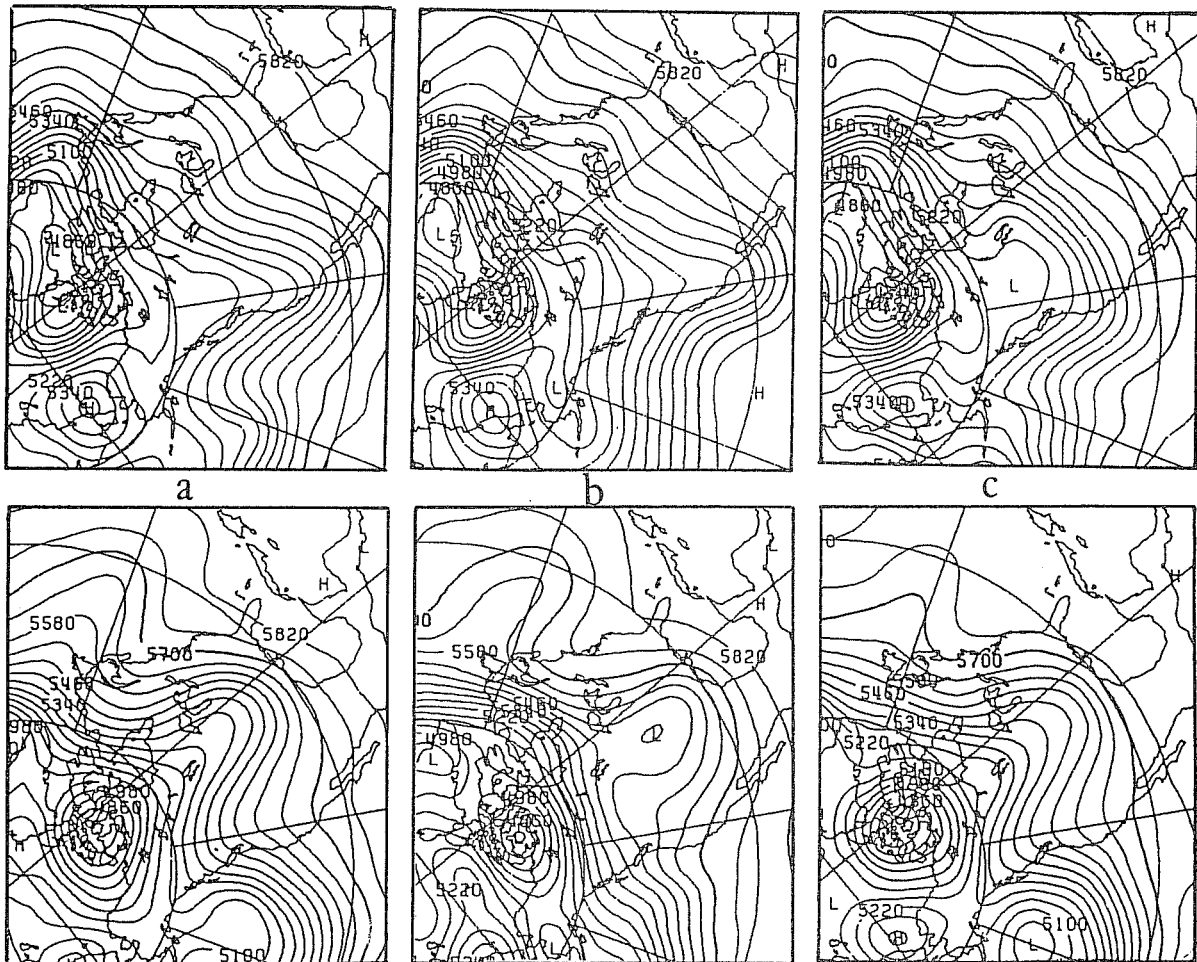Fig.23　The same as Fig.19 except 120hr sea level pressure.

Fig.24　500mb height forecast (CONTL (a), NOSAT (c)) on the basis of
analysis at 00GMT 28 February and verification (b).
top (48 hours), bottom (96 hours)

In certain situations differences in initial analyses move in accordance with the movement of systems (trough or ridge), but in other situations areas of large differences propagate with a faster speed than that of the system. Also the duration varies case by case. Further dynamical studies are needed to clarify how and in what situations the above mentioned differences are caused.

9. CONCLUSION

(1)   The JMA analysis system is designed so that it fully utilizes the satellite data; in other words, analysis quality depends greatly on the availability of satellite data. Since the system adopts a two-dimensional analysis procedure, vertical consistency is more sensitive to SATEM data availability than in a three-dimensional analysis. Accordingly, when all types of data are available, conventional data and space based data are properly mixed to yield a stable and high quality analysis.

(2)   Space based data are indispensable in low latitudes and the southern hemisphere where conventional data are sparse.

(3)   Even in the northern hemisphere, erroneous analyses are produced in the Pacific region in the stratosphere when we exclude satellite data. This is considered to be due to the use of a wavenumber in the stratospheric analysis which is not suitable for fitting the data distribution. The analysis errors in the stratosphere gradually propagate into the troposphere through the assimilation cycles.

(4)   The results mentioned in (3) indicate the limitation of observing system experiments using a system based on the present full data coverage. The parameters of the analysis system (e.g. wave number and forecast error) should be modified according to the data available.

(5)   In the troposphere also, satellite data exhibit a strong impact on analyses over the Pacific region. The impact at a certain time level naturally appears as the sum of the impact of data existing at that time level and the impact of data from previous time levels evolved through the assimilation system.

(6)   Both the statistical and synoptic evaluations indicate that satellite

data improves the analysis over the Pacific and thereby improves the forecast

over North America.   On the other hand, analysis improvements due to satellite

data has little impact on the forecast around East Asia because sonde data

basically determines the quality of the analysis upstream of that region.

(7)   The duration or propagation of differences in the analysis field in the

course of a forecast are not the same for all the cases investigated.   Further

dynamical studies are needed to clarify why this occurs.

References

Alaka, M.A. and R.C. Elvander, 1972: Optimum interpolation from observation of mixed quality. Mon.Wea.Rev., 100, 612-624.

Begman, K.H., 1979: Multivariate analysis of temperatures and winds using optimum interpolation. Mon.Wea.Rev., 107, 1423-1444.

Kanamitsu, M., et al., 1983: Description of the JMA operational spectral model. J.Met.Soc.Japan, 61, 812-838.

Kurihara, Y., 1961: Accuracy of winds-aloft data and estimation of error in numerical analysis of atmospheric motions. J.Met.Soc.Japan, 39, 331-345.

Lenhard, R.W., 1970: Accuracy of radiosonde temperature and pressure height determination. Bull.Amer.Met.Soc., 51, 842-846.